

Theta Oscillations in Somata and Dendrites of Hippocampal Pyramidal Cells In Vivo: Activity-Dependent Phase-Precession of Action Potentials

Anita Kamondi,^{1,2} László Acsády,^{1,3} Xiao-Jing Wang,⁴ and György Buzsáki^{1*}

¹Center for Molecular and Behavioral Neuroscience, Rutgers University, Newark, New Jersey

²Department of Neurology, Semmelweis University, Medical School, Budapest, Hungary

³Institute of Experimental Medicine, Hungarian Academy of Sciences, Budapest, Hungary

⁴Volen Center for Complex Systems, Brandeis University, Waltham, Massachusetts

ABSTRACT: Theta frequency field oscillation reflects synchronized synaptic potentials that entrain the discharge of neuronal populations within the ~100–200 ms range. The cellular-synaptic generation of theta activity in the hippocampus was investigated by intracellular recordings from the somata and dendrites of CA1 pyramidal cells in urethane-anesthetized rats. The recorded neurons were verified by intracellular injection of biocytin. Transition from non-theta to theta state was characterized by a large decrease in the input resistance of the neuron (39% in the soma), tonic somatic hyperpolarization and dendritic depolarization. The probability of pyramidal cell discharge, as measured in single cells and from a population of extracellularly recorded units, was highest at or slightly after the negative peak of the field theta recorded from the pyramidal layer. In contrast, cyclic depolarizations in dendrites corresponded to the positive phase of the pyramidal layer field theta (i.e. the hyperpolarizing phase of somatic theta). Current-induced depolarization of the dendrite triggered large amplitude slow spikes (putative Ca²⁺ spikes) which were phase-locked to the positive phase of field theta. In the absence of background theta, strong dendritic depolarization by current injection led to large amplitude, self-sustained oscillation in the theta frequency range. Depolarization of the neuron resulted in a voltage-dependent phase precession of the action potentials. The voltage-dependent phase-precession was replicated by a two-compartment conductance model. Using an active (bursting) dendritic compartment spike phase advancement of action potentials, relative to the somatic theta rhythm, occurred up to 360 degrees. These data indicate that distal dendritic depolarization of the pyramidal cell by the entorhinal input during theta overlaps in time with somatic hyperpolarization. As a result, most pyramidal cells are either silent or discharge with single spikes on the negative portion of local field theta (i.e., when the somatic region is least polarized). However, strong dendritic excitation may overcome perisomatic inhibition and the large depolarizing theta rhythm in the dendrites

may induce spike bursts at an earlier phase of the extracellular theta cycle. The magnitude of dendritic depolarization is reflected by the timing of action potentials within the theta cycle. We hypothesize that the competition between the out-of-phase theta oscillation in the soma and dendrite is responsible for the advancement of spike discharges observed in the behaving animal. *Hippocampus* 1998;8:244–261.

© 1998 Wiley-Liss, Inc.

KEY WORDS: dendrites; input resistance; spike timing; temporal coding; inhibition; resonance; network

INTRODUCTION

Synchronization of neurons to local field oscillations has been demonstrated in many neural networks (Buzsáki et al., 1983; Gray et al., 1989; Singer, 1993; Bragin et al., 1995; Ylinen et al., 1995a,b; Laurent, 1996; Steriade et al., 1996). Such entrainment mechanisms are the means for bringing neuronal aggregates within/across structures together in time, so as to act in concert. During hippocampal theta waves, associated with exploratory locomotion and REM sleep (Vanderwolf, 1969), neurons within the entorhinal-hippocampal input network discharge in an organized manner (Mitchell and Ranck, 1980; Buzsáki et al., 1983; Alonso and Garcia-Austts, 1987; Chrobak and Buzsáki, 1997).

Despite the fact that theta oscillation is a prominent field pattern and occurs in an architectonically simple cortical structure, its generation and function are not fully understood (Bland, 1986; Stewart and Fox, 1990; Buzsáki et al., 1994). The rhythm generator of hippocam-

Grant sponsor: NIH; Grant numbers: NS34994; MH54671; MH53717; Grant sponsors: Alfred P. Sloan Foundation; Human Frontier Science Program; Soros Foundation; Whitehall Foundation.

*Correspondence to: György Buzsáki, Center for Molecular and Behavioral Neuroscience, Rutgers University, Newark, NJ 07102.

E-mail: buzasaki@axon.rutgers.edu

Accepted for publication 3 March 1998

pal-entorhinal theta oscillation is the medial septum and the vertical limb of the diagonal band of Broca (Petsche et al., 1962). Cholinergic cells of the septal region innervate both principal cells and interneurons of the hippocampus (Leranth and Frotscher, 1987), whereas the septohippocampal GABAergic projection terminates predominantly on interneurons (Freund and Antal, 1988). Extracellular studies suggest that the main current generators of field theta waves are the coherent dendritic and somatic membrane potential fluctuations of the orderly aligned pyramidal cells and granule cells (Winson, 1974; Bland et al., 1975; Buzsáki et al., 1983, 1986; Brankack et al., 1993). In the intact rat, theta activity is characterized by a gradual phase-shift with depth from the pyramidal layer to the distal apical dendrites, and a large amplitude peak at the level of the hippocampal fissure. Under urethane or ketamine anesthesia the phase reversal is steeper and the theta amplitude is significantly smaller, especially at the level of the hippocampal fissure. The depth profile of theta activity under anesthesia in many ways resembles the theta profile following entorhinal cortex lesion. These studies have led to the hypothesis that a large part of the extracellular currents underlying field theta derive from rhythmic excitation of the distal dendrites by the perforant path input (Winson, 1974; Buzsáki et al., 1983; Leung, 1984; Buzsáki et al., 1986; Boeijinga and Lopes da Silva, 1989; Lopes da Silva et al., 1990; Brankack et al., 1993; Soltész and Deschênes, 1993; Ylinen et al., 1995b). Direct support for somatic hyperpolarization during theta is available from studies which investigated the intrasomatic correlates of theta waves in pyramidal cells and interneurons (Fujita and Sato, 1964; Artemenko, 1972; Leung and Yim, 1986; Fox, 1989; Nuñez et al., 1987, 1990; Konopacki et al., 1992; Soltész and Deschênes, 1993; Ylinen et al., 1995b). On the other hand, no information is available about the behavior of dendritic membranes during theta activity.

Whereas previous studies focused on the "average" relationship between field oscillations and cellular firing, recent observations indicate that timing within the theta cycle may be an important mechanism for representing neuronal information (O'Keefe and Recce, 1993; Skaggs et al., 1996). Hippocampal pyramidal cells possess "place fields," i.e., they selectively increase their firing rates when the rat is in a specific part of the environment (O'Keefe and Nadel, 1978). Whereas previous cross-correlation studies have shown that pyramidal cells discharge mostly on the negative phase of the locally derived theta (Buzsáki et al., 1983; Fox et al., 1986; Skaggs et al., 1986), O'Keefe and Recce (1993) noticed that sequentially occurring spikes gradually shift to earlier phases of the theta cycle as the rat approaches and passes through the cell's place field. Importantly, the phase relationship of the spike to theta cycle was a good predictor of the rat's position in space. Several models have attempted to explain this phase precession but the physiological mechanism has remained unknown. The issue is important because understanding the physiological basis of this behaviorally relevant phenomenon could provide some insight about the neuronal representation of information.

To advance the above issues we examined the intracellular events of field theta activity in the somata and dendrites of CA1 hippocampal pyramidal cells. Four main issues were addressed.

First, we examined the nature of intradendritic activity during theta. Second, we compared the cell's input resistance and the polarization changes of the membrane in the soma and dendrites during theta and non-theta states. Third, we asked whether intrinsic properties of dendrites can contribute to the theta cycles. Finally, we explored the possible sources of theta phase precession of action potentials in both experiments and computer simulation.

MATERIALS AND METHODS

Forty-six rats of the Sprague-Dawley strain (250–350 g) were anesthetized with urethane (1.3–1.5 g/kg) and placed in a stereotaxic apparatus. Body temperature was kept constant by a small animal thermoregulation device. The scalp was removed and a small (1.2 / 0.8 mm) bone window was drilled above the hippocampus (anteromedial edge at AP = -3.3 and L = 2.2 mm from bregma) for extra- and intracellular recordings. The cisterna magna was opened and the cerebrospinal fluid was drained to decrease pulsation of the brain. A pair of stimulating electrodes (100 μ m each, with 0.5 mm tip separation) was inserted into the left fimbria-fornix (AP = -1.3, L = 1.0, V = 4.1) to stimulate the commissural inputs. Another pair of stimulating electrodes was placed into the perforant path (AP = -6.5, L = 4.5, V = 4.0). Extracellular recording electrodes (two 20- μ m insulated tungsten wires) were inserted at the medial edge of the bone window and placed into the CA1 pyramidal layer and the hilus, respectively. Positioning of the recording electrode in the CA1 pyramidal layer was aided by the presence of multiple unit activity and the commissurally evoked responses. The hilar position of the recording electrode was determined by the distance (>200 μ m) from the polarity reversal of the perforant path-evoked response. After the extracellular and intracellular recordings electrodes were inserted into the brain, and the bone window was covered by a mixture of paraffin and paraffin oil to prevent drying of the brain and decrease pulsation. The distance of the intracellular and extracellular electrodes was 0.5–1.5 mm in the anteroposterior and 0.0–0.5 mm in the lateral directions (Penttonen et al., 1997).

Micropipettes for intracellular recordings were pulled from 2.0-mm capillary glass. They were filled with 1 M potassium acetate in 50 mM Tris buffer (pH 7.2), also containing 2% biocytin for intracellular labeling. In some experiments the recording pipette also contained 10 mM of the lidocaine derivative QX 314 (Sigma, St. Louis, MO). The intracellular electrode was inserted <1.0 mm posterior to the extracellular electrodes. In vivo electrode impedances varied from 60 to 100 M Ω . Once stable intracellular recordings were obtained, evoked and passive physiological properties of the cell were determined. Only neurons with a resting potential more negative than -55 mV were included in this study. Since the "resting" membrane potential fluctuates in vivo, we used the amplifier's (Axoclamp-2B; Axon Instruments, Foster City, CA) voltmeter readings to obtain an average value integrated over time. The input resistance of

neurons was calculated from steady state membrane responses to hyperpolarizing and depolarizing current steps. A linear regression was fitted to these values.

Field activity recorded through the extracellular electrode was filtered between 1 Hz and 5 kHz. The intracellular activity and the extracellular field/unit activity were digitized at 10 kHz with 12-bit precision (R. C. Electronics, Santa Barbara, CA). The electrophysiological data were stored on optical disks. The data were analyzed off-line. The extracellular trace was digitally filtered at 120 dB/octave in order to select the frequency of interest: theta waves (2.5–7 Hz) and unit activity (500 Hz–5 kHz) using fast Fourier transformation (FFT). Extracellular units were detected by an amplitude discriminator software.

All recordings in this study were made from biocytin-injected and morphologically identified CA1 pyramidal cells. When a biocytin injection of a single cell resulted in labeling two or more neurons, the physiological data obtained from these recordings were discarded from the analysis. After the completion of the physiological data collection biocytin was injected through a bridge circuit using 500-ms depolarizing pulses at 0.6–2 nA at 1 Hz for 10–60 min. Neuronal activity was followed throughout the procedure and the current was reduced if the electrode was blocked and/or the condition of the neuron deteriorated. Two to 12 hours after the injection the animals were given an urethane overdose and then perfused intracardially with 100 ml physiological saline followed by 400 ml of 4% paraformaldehyde and 0.2% glutaraldehyde dissolved in phosphate buffered saline (pH 7.2). The brains were then removed and stored in the fixative solution overnight. Coronal sections, 60 or 100 μm thick, were cut and processed for biocytin labeling. The labeled neurons were reconstructed with the aid of a drawing tube. The histological sections were also used to verify the position of the extracellular recording electrodes and the track made by the recording pipette (Sik et al., 1995).

The data for the current-source density (CSD) analysis presented here were obtained from an earlier study (Ylinen et al., 1995a). CSD analysis provides a more precise localization for the origin of extracellular currents than depth profile of voltage distribution (Mitzdorf, 1985). When extracellular potentials are simultaneously measured at various depths, the CSD derivatives of the voltage traces allow for the continuous monitoring of the exact anatomical locations of sinks and sources. For the construction of CSD plots (CSD vs. time), theta waves were averaged ($n = 100$ to 200). The results are presented as the unscaled second derivative of potential as a function of depth (Bragin et al., 1995). The exact anatomical layers corresponding to the vertical scale of the CSD maps were reconstructed with the aid of the histologically identified recording tracks and thalamic-evoked potentials.

For dendritic recordings the tip of the recording electrode was determined by both physiological and histological methods. Following the withdrawal of the pipette from the dendrite, extracellular averaged evoked responses to commissural stimulation were obtained at 50- μm steps from the recording site to the pyramidal layer. The polarity reversal of the extracellular field response at the border of strata radiatum and pyramidale provided an additional landmark for the pyramidal layer. The location of

dendritic penetration was determined from the distance between the pyramidal layer and the recording site during the experiment and from the anatomical reconstruction of the electrode track and the dendritic tree of the filled neuron. The pipette was moved up and down several times after its withdrawal from the cell to facilitate histological reconstruction of the electrode track.

Computer Model

Computer simulations were carried out with a model of CA1 pyramidal neurons. The model is minimal for our purpose, with two compartments representing the soma and dendrite, respectively (Pinsky and Rinzel, 1994). It is well known that both voltage-gated Ca^{2+} and Na^+ currents are involved in active responsiveness of CA1 pyramidal dendrites (Wong et al., 1979; Andreassen and Lambert, 1995; Jensen et al., 1996). Our minimal model contains a persistent Na^+ current I_{NaP} , as suggested by data from CA1 pyramidal neurons (Jensen et al., 1996), as well as a voltage-gated slowly activating K^+ current I_{KS} to counterbalance I_{NaP} . For the sake of simplicity, however, it does not include voltage-gated Ca^{2+} currents and Ca^{2+} -activated K^+ currents, unlike the widely used pyramidal cell models (Pinsky and Rinzel, 1994; Traub et al., 1994; Wang, 1988). The somatic compartment contains spike-generating currents I_{Na} and I_{K} , while the dendritic compartment has an I_{NaP} and an I_{KS} . The somatic and dendritic membrane potentials V_s and V_d obey the following current-balance equations:

$$C_m \frac{dV_s}{dt} = -I_L - I_{\text{Na}} - I_{\text{K}} - \frac{g_c}{p} (V_s - V_d) + I_{\text{soma}}; \quad (1)$$

$$C_m \frac{dV_d}{dt} = -I_L - I_{\text{NaP}} - I_{\text{KS}} - \frac{g_c}{(1-p)} (V_d - V_s) + I_{\text{dendrite}} \quad (2)$$

where $C_m = 1 \mu\text{F}/\text{cm}^2$; I_{soma} and I_{dendrite} are the injected currents to the soma and dendrite, respectively. Following Pinsky and Rinzel (1994), we express the current flows between the soma and dendrite [proportional to $(V_s - V_d)$] in $\mu\text{A}/\text{cm}^2$, with the coupling conductance $g_c = 1 \text{ mS}/\text{cm}^2$ and the parameter $p = \text{somatic area}/\text{total area} = 0.15$. The leak current $I_L = g_L(V - V_L)$, while the voltage-dependent currents are described by the Hodgkin-Huxley formalism. Thus, a gating variable x satisfies a first-order kinetics,

$$dx/dt = \phi_x(\alpha_x(V)(1-x) - \beta_x(V)x) = \phi_x(x_\infty(V) - x)/\tau_x(V) \quad (3)$$

The persistent Na^+ current $I_{\text{NaP}} = g_{\text{NaP}} m_\infty^3 (V - V_{\text{Na}})$, where the fast activation is substituted by its steady state $m_\infty(V) = 1/(1 + \exp(-(V + 57.7)/7.7))$ (Galue and Alonso, 1996). The slow K^+ current $I_{\text{KS}} = g_{\text{KS}} m(V - V_{\text{K}})$, with $m_\infty(V) = 1/(1 + \exp(-(V + 35)/6.5))$ and $\tau_m(V) = 200/(\exp(-(V + 55)/30) + \exp((V + 55)/30))$. The sodium current $I_{\text{Na}} = g_{\text{Na}} m^3 h(V - V_{\text{Na}})$, with $\alpha_m = -0.1(V + 31)/(\exp(-0.1(V + 31)) - 1)$, $\beta_m = 4\exp(-(V + 56)/18)$; $\alpha_h = 0.07\exp(-(V + 47)/20)$, and $\beta_h = 1/(\exp(-0.1(V + 17)) + 1)$. The delayed rectifier $I_{\text{K}} = g_{\text{K}} n^4 (V - V_{\text{K}})$, with $\alpha_n = -0.01(V + 34)/(\exp(-0.1(V + 34)) - 1)$, and $\beta_n = 0.125\exp(-(V + 44)/80)$. The temperature factors $\phi_m = 10$, $\phi_h = \phi_n = 3.33$. Other parameter

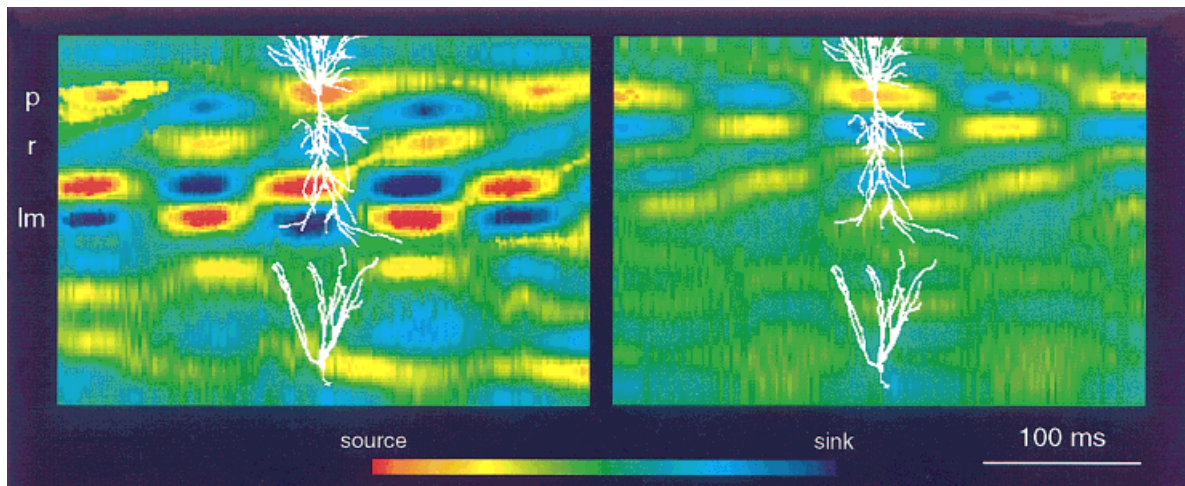


FIGURE 1. Extracellular current flow during theta waves in the awake, exploring rat. The simultaneously obtained field potentials (recorded by 16 equally spaced sites parallel to the dendrites of pyramidal cells at 100- μ m intervals) were converted to one-dimensional CSD maps. Left: Intact animal. Approximately two theta cycles are shown. During the positive portion of the extracellularly recorded theta waves in the pyramidal layer (p), rhythmic sinks

(blue) in the stratum lacunosum-moleculare are coupled to rhythmic sources (red) in the pyramidal layer. Right: Same animal after bilateral removal of the entorhinal cortex. Note the survival of the perisomatic source in the pyramidal layer and the absence of the sink-source pair in the distal dendrites. (Original voltage data are from Ylinen et al., 1995b.) The same time and color scales apply to both CSD maps.

values are: $g_L = 0.18$, $g_{NAP} = 0.05$, $g_{KS} = 1.4$, $g_{Na} = 55$, $g_K = 20$ (in mS/cm²); $V_L = -65$, $V_{Na} = +55$, $V_K = -90$ (in mV).

RESULTS

Inference of Distal Dendritic Excitation From Extracellular Field Recordings

Previous experiments using extracellular recording methods have already pointed to the importance of the entorhinal input in theta generation. In the intact rat, theta activity is characterized by a gradual phase-shift with depth from the pyramidal layer to the distal apical dendrites, a large amplitude peak at the level of the hippocampal fissure and high coherence at all depths. These previous experimental and modeling (Winson, 1974; Buzsáki et al., 1983; Leung, 1984; Buzsáki et al., 1986; Lopes da Silva et al., 1990; Brankack et al., 1993) studies have indicated that a large part of the extracellular currents underlying field theta derive from rhythmic excitation of the distal dendrites by the perforant path input. The distribution of the main theta dipoles is illustrated by the current-source density (CSD) map of the extracellular charges (Fig. 1). Confirming previous observations, the theta-associated source at the pyramidal cell layer is associated with a large sink localized to the stratum lacunosum-moleculare of the intact animal. The critical role of the entorhinal input is also illustrated. After removal of the entorhinal input in the same animal, the sink-source pair around stratum lacunosum-moleculare virtually disappeared.

In contrast to the above observations, the intracellular experiments presented below were performed under anesthesia. This is a caveat because the depth profile of theta under urethane and

ketamine anesthesia in many respects is similar to that observed after removing the entorhinal input (Soltész and Deschênes, 1993; Ylinen et al., 1995b). It may be that both types of anesthetics interfere with glutamate-receptor mediated transmission. Therefore, it should be kept in mind that dendritic excitation under anesthesia is considerably weaker than in the awake, drug-free animal.

Properties of Somatic and Dendritic Activity in CA1 Pyramidal Neurons

The contributions of somatic and dendritic activity of CA1 pyramidal cells to sharp waves and gamma waves have been previously described in an overlapping set of animals (Penttonen et al., 1988; Kamondi et al., in press). Passive properties of soma and dendrites of neurons in the present study are shown in Table 1. Similar to in vitro observations, depolarizing pulses in dendrites evoked a train of action potentials with progressively decrementing amplitude (Spruston et al., 1995; Tsubokawa and Ross, 1996; Hoffman et al., 1997). Larger current steps induced a large amplitude slow spike, likely reflecting high-threshold Ca²⁺ currents (Wong et al., 1979; Wong and Stewart, 1992; Magee and Johnston, 1995) and an associated burst of fast spikes (e.g., Fig. 8B). The amplitude of spontaneous fast action potentials in the apical dendrites was always smaller than those recorded from the soma and decreased as a function of the distance from the pyramidal layer (Spruston et al., 1995; Hoffman et al., 1997; Kamondi et al., in press). The rate of rise and decay, the width at half-amplitude, and the spike afterpotential also correlated with the location of the dendritic recording (Table 1). Passive properties of somatic recordings were similar to those reported earlier for sharp electrodes in vivo (Leung and Yim, 1986; Soltész and Deschênes, 1993; Ylinen et al., 1995b).

TABLE 1.

Properties of Somatic and Dendritic Action Potentials

	Soma	Proximal	Middle	Distal
Spike A (mV)	62.2 ± 5.8	44.1 ± 7.2	28.7 ± 12.7	8.8 ± 7.2
Rise rate (V/s)	100.1 ± 22.8	72.7 ± 20.4	40.1 ± 22.2	10.7 ± 10.4
Decay rate (V/s)	55.9 ± 9.4	33.7 ± 9.2	18.8 ± 13.5	3.2 ± 3.5
Half-A width (ms)	0.9 ± 0.07	1.1 ± 0.17	1.5 ± 0.8	2.9 ± 1.5
RMP (mV)	61.2 ± 5.4	66.4 ± 4.9	66.1 ± 4.2	65.1 ± 3.9
Spike AP (mV)	-3.65 ± -2.7	5 ± 2.5	6.2 ± 2.2	3.9 ± 2.1
Input _R (MΩ)	30.4 ± 6.2	27.7 ± 3.3	23.1 ± 2.2	19.9 ± 2.0

Dendritic recordings were arbitrarily divided into three equal parts: proximal, middle and distal thirds of stratum radiatum.

Spike A, amplitude of action potentials (measured from the inflection point to the peak).

Rise rate, rate of rise of action potential.

Decay rate, rate of decay of action potential.

Half-A width, width of the action potential at half amplitude.

RMP, resting membrane potential.

Spike AP, fast spike after polarization.

Input_R, input resistance.

All values are mean ± standard error ($n_{\text{soma}} = 35$, $n_{\text{dendrite}} = 56$).

(Pooled data from the present study, Penttonen et al., 1998, and Kamondi et al., 1998).

Hyperpolarization and Shunting of Somatic Membrane During Theta Activity

In agreement with previous reports (Artemenko, 1972; Leung and Yim, 1986; Nuñez et al., 1987; Fox, 1989; Nuñez et al., 1990; Konopacki et al., 1992; Soltész and Deschénes, 1993; Ylinen et al., 1995b), intrasomatic recordings from CA1 pyramidal neurons revealed membrane potential oscillations which were coherent with the extracellularly recorded theta EEG (Fig. 2). The mean intracellular voltage fluctuation varied from 2 to 9.5 mV at resting membrane potential ($n = 30$ cells). When theta activity was evoked by tail pinching or emerged spontaneously from an irregular background, the soma of the pyramidal cell became tonically hyperpolarized (2 to 10 mV) and the intracellular oscillation only rarely reached depolarization levels of action potential generation. The extracellular field theta recorded in the pyramidal cell layer and the intracellularly recorded oscillation were out of phase, and the action potential of the pyramidal neurons, on average, occurred near the negative peak of the locally derived extracellular theta.

The input resistance of the soma was monitored by small hyperpolarizing current steps (-0.2 nA; 70–300 ms). The input resistance varied dynamically and depended strongly on the background activity. When theta activity occurred spontaneously or was evoked by tail pinching, the input resistance decreased by 39%, on average (Fig. 3; non-theta, 44.1 ± 7.22 MΩ; theta, 24.3 ± 6.46 MΩ; $n = 12$ cells; $t = 2.53$; $P < 0.01$). This effective shunting of the somatic domain may have been brought about by basket and chandelier cell-mediated GABA_A inhibition (Cobb et al., 1995; Ylinen et al., 1995b). Support of the shunting hypothesis was provided by the observation that the amplitude of evoked somatic action potentials was always smaller ($26.1 \pm$

4.41% ; $n = 32$; $t = 5.42$; $P < 0.001$) than that of the spontaneously occurring ones (Fig. 3D). In the latter case, shunting was induced by the feed-forward activation of basket cells by the commissural input. Theta-induced hyperpolarization and reduction of the somatic input resistance were consistently present in all cells tested independent of whether the recording pipette contained QX 314 (three cells), a lidocaine derivative to block the fast sodium spikes (Connors and Prince, 1982; Nathan et al., 1990; Andrade, 1991), or not (nine cells; Fig. 2B).

Phase-Advancement of Action Potentials in the Theta Cycle

Theoretical models have suggested that information represented by neuronal activity is reflected by the phase-relation of spike occurrence relative to the population cycle (Buzsáki and Chrobak, 1995; Hopfield, 1995; Lisman and Idiart, 1995; Laurent, 1996; Tsodyks et al., 1996). It was demonstrated experimentally that the timing of the extracellularly recorded units shows a gradual phase-shift when the rat traverses the spatial field represented by that neuron (O'Keefe and Recce, 1993; Skaggs et al., 1996).

Because "place" cells are likely to be excited most by their afferents in the center of the field, we hypothesized that it is this "ramp-like" depolarization superimposed on the background theta activity which causes the pyramidal cells to fire progressively earlier during the theta cycle. We tested this hypothesis by imposing a cyclic oscillation on the somatic membrane by current injection at theta frequency combined with increasing levels of depolarization (Fig. 4). A small sinusoid current at resting membrane potential caused an irregular discharge of the cell coinciding with its depolarizing phase, similar to what is observed during network-induced theta (Ylinen et al., 1995b). Shifting the

Somatic recording

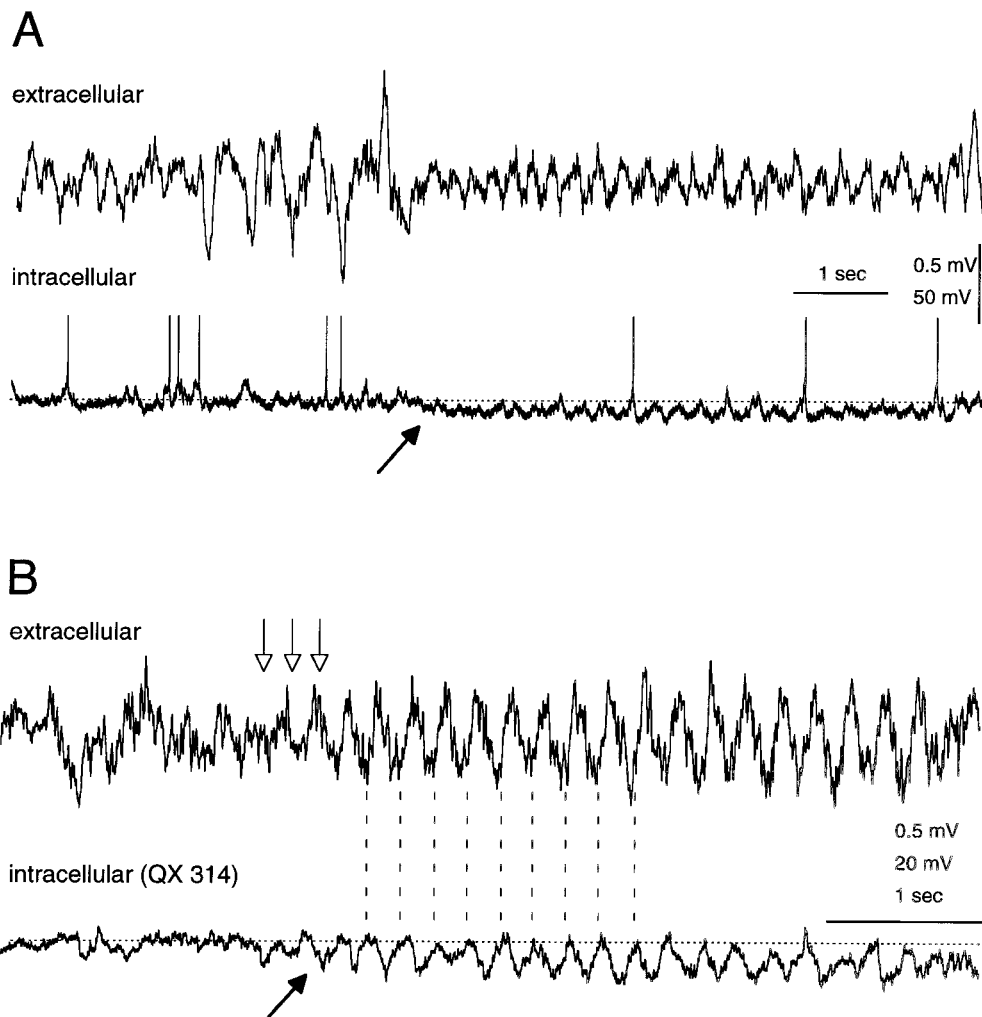


FIGURE 2. Theta is associated with somatic hyperpolarization. **A:** Simultaneous recording of extracellular EEG activity in the CA1 pyramidal layer (extracellular) and intracellular activity of a pyramidal cell in the urethane-anesthetized rat. Note rhythmic membrane oscillation in the hyperpolarizing direction of the pyramidal cell at the onset of spontaneous theta activity (arrow). Action potentials are

clipped. Dotted line represents -60 mV, "resting" potential. **B:** Similar experiment to A but the recording pipette contained QX 314 to block Na^+ spikes (10 mM). Theta activity was induced by tail pinching (three empty arrows). Dashed lines indicate that the peak of the intracellular theta cycle corresponds to the negative phase of the locally derived extracellular theta in the CA1 pyramidal layer.

membrane potential to more positive values resulted in a higher frequency discharge of the cell and advancement of the occurrence of the first spike as well as an advancement of the peak firing rate relative to the peak depolarization ($n = 9$ cells). Depolarization of the neurons to -40 – 50 mV resulted in the regular occurrence of the first spike in the trough of the oscillation, corresponding to 120 to 180 degrees of phase advancement of the action potential (Fig. 4; -45 mV). The peak firing rate also showed a phase precession but usually not more than 90 degrees. The distribution of spikes was asymmetrical relative to the intracellular theta cycle. Most of the action potentials occurred during the rising phase of theta. Action potentials on the falling phase (positive to negative going) of the induced theta, similar to spontaneous intracellular theta waves, were less frequent. Depolarization of the soma to

more positive values resulted in broadening of the spikes and partial or complete depolarization blockade of the action potentials. In summary, theta frequency modulation, coupled with tonic depolarization in the soma, replicated some features of phase-precession in the behaving animal. However, it failed to produce phase advancement more than 180 degrees, observed experimentally (O'Keefe and Recce, 1993; Skaggs et al., 1996).

Modeling of Depolarization-dependent Phase-shift of Action Potentials

Due to the constraints of the *in vivo* method, simultaneous recordings from the soma and dendrite of the same pyramidal cell were not performed. As an alternative, the contribution of

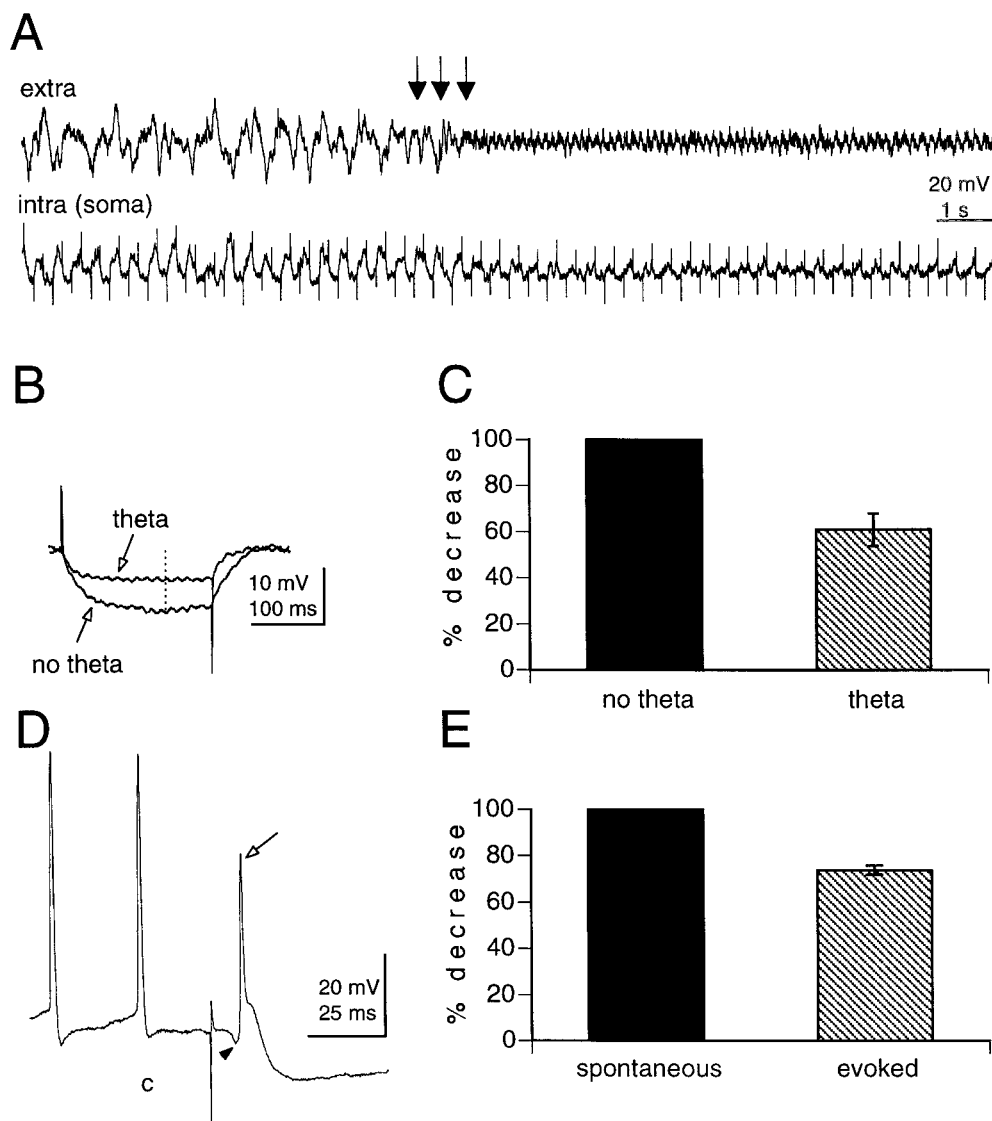


FIGURE 3. Somatic input resistance decreases during theta activity. **A:** Simultaneous extracellular (extra) and intrasomatic (intra) recordings during non-theta to theta transition. Arrows indicate tail pinch. The input resistance of the cell was tested by hyperpolarizing current pulses (-0.2 nA; 250 ms). Note rapid and large decrease of the input resistance of the cell at theta onset. **B:** Averaged voltage responses to the hyperpolarizing pulses. The input resistance of the neuron decreased from 58.4 M Ω (non-theta) to 22.6 M Ω (theta). Dotted line

represents time of amplitude measurement. **C:** Group averages of input impedance values in CA1 pyramidal cell somata ($n = 12$). Ordinate, percentage decrease of input resistance. **D:** Monosynaptically evoked action potential in response to commissural stimulation (c). Arrowhead indicates early hyperpolarization (feed-forward inhibition). Note that the amplitude of the evoked spike (arrow) is reduced relative to the preceding spontaneous action potentials. **E:** Group averages ($n = 32$ cells). Ordinate, percentage decrease of amplitude.

dendritic depolarization to the phase advancement of action potentials was simulated by a two-compartment (soma and dendrite) model (Fig. 5). A sinusoidal current was applied to the soma, which by itself was not sufficient for the cell to reach the firing threshold. Additional dendritic depolarization discharged the cell but, in the absence of slow active currents I_{NaP} and I_{KS} , did not induce a systematic phase advancement. Instead, action potentials occurred symmetrically with respect to the peak of the cycle, and the average firing was centered at the peak of the input current (data not shown). The addition of the slow K^+ current I_{KS} , however, induced asymmetrical discharge during theta cycle. With weak excitation by a constant current injection to the dendrite

$I_{dendrite}$ the cell began to emit action potentials at the peaks of the oscillatory input to the soma. With gradual increase of $I_{dendrite}$, the cell could reach the firing threshold at an earlier phase of the cycle, and there were more spikes per cycle. Because during the rising phase of the cycle the slow K^+ current I_{KS} was gradually activated, it reduced the excitability of the cell for the rest of the cycle. As a result, spike discharges were mostly confined to the rising phase, similar to our experimental observations (Fig. 4). This indicated that there is a net advancement of firing times with respect to the somatic input cycle, as the tonic dendritic drive is increased. Spike discharges were occasionally observed on the falling phase of the theta cycle, depending on the model parameters or applied current

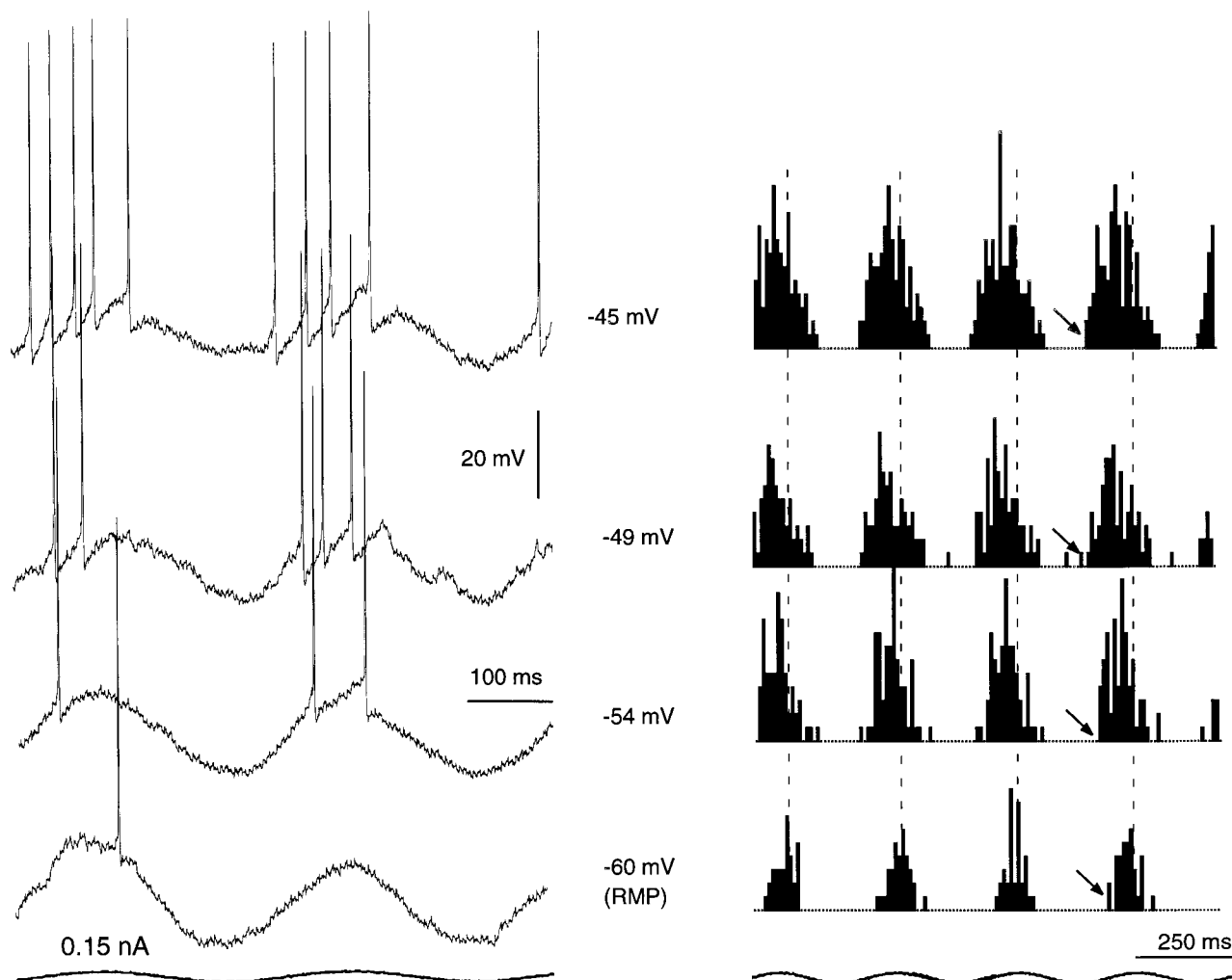


FIGURE 4. Phase advancement of action potentials. Left: Somatic membrane responses to sinusoid current (0.15 nA). In addition the soma was depolarized to various voltage levels by an additional DC current to voltage levels indicated on the right of the traces. Note that most action potentials were emitted on the rising phase of oscillation and that the first

action potential occurred progressively earlier upon increasing levels of depolarization. Right: Averaged histograms of action potentials. Both the first action potentials (arrows) and the average peak firing (vertical dashed lines) occurred at an earlier phase of the oscillation upon depolarization. RMP, resting membrane potential.

intensities. However, in all cases there was a clear asymmetry of firing patterns with respect to the peak of the cycle, due to the slow I_{KS} . Somatic theta frequency oscillation, coupled with tonic dendritic depolarization, however, failed to produce spike phase advancement more than 180 degrees.

Intradendritic Correlates of Theta Oscillation in Pyramidal Cells

Theta-related membrane potential changes were also observed in the dendrites of pyramidal cells. In contrast to the soma, the onset of theta activity was accompanied by a steady depolarization of the dendritic membrane (Fig. 6). The magnitude of theta-associated steady depolarization in the dendrites recorded at sites $>200 \mu\text{m}$ from the somatic layer varied from 2 to 12 mV ($n = 6$ cells). In two proximal recording sites ($<200 \mu\text{m}$ from the pyramidal layer) no voltage shift was observed and in another proximal site a small hyperpolarization (3 mV) was present. The

steady depolarization of the membrane at the onset of theta activity was accompanied by an amplitude decrease of dendritic spikes. In the presence of theta activity, the amplitude of action potentials was relatively uniform. In the absence of theta, on the other hand, the amplitude varied extensively in distal dendrites. Large amplitude action potentials (>50 mV) were also observed, typically in association with sharp wave-associated "ripple" oscillation and multiple unit bursts in the extracellular recording site (Kamondi et al., in press). The relative amplitude increase during non-theta as compared to theta epochs is illustrated in Figure 6C. The input resistance of the dendrite also decreased during theta activity. However, the magnitude of this decrease was less (0%, 7%, 11% and 11%, in four cells, respectively) than measured in the soma.

Similar to intracellular theta recorded in the soma (Nuñez et al., 1987; Fox, 1989; Soltész and Deschênes, 1993; Ylinen et al., 1995b), theta oscillation of the dendritic membrane potential was voltage-dependent. Steady depolarization of the membrane by

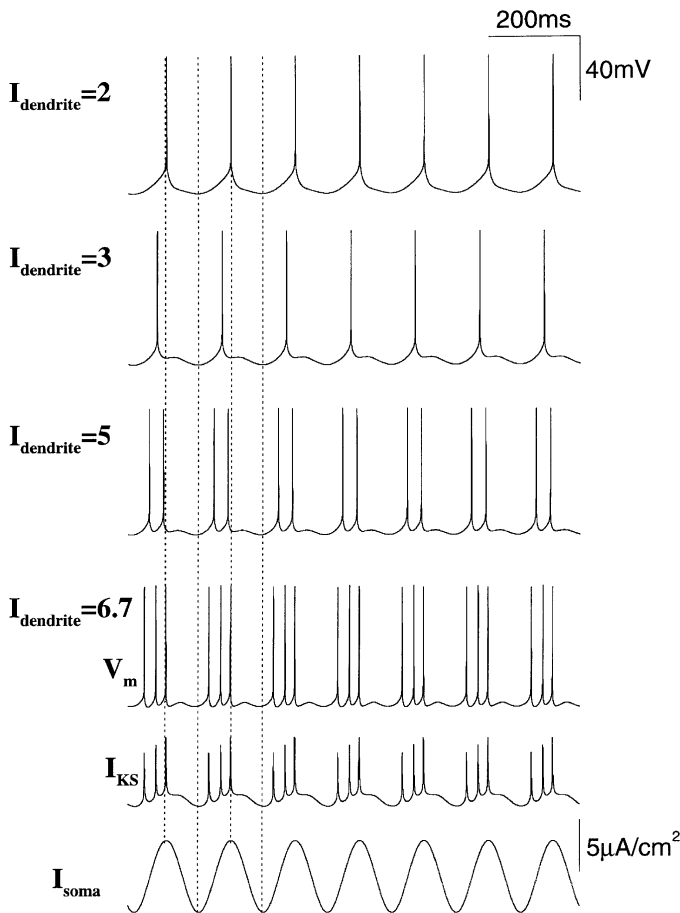


FIGURE 5. Computer simulation of theta phase advancement of the action potential by a two-compartment conductance-based model. Bottom trace: Sinusoidal current applied to the soma at 7 Hz. Without simultaneous current injection to the dendrite the model neuron does not discharge (not shown). With small I_{dendrite} , the soma fires at the peak of I_{soma} . Stronger I_{dendrite} produces a gradual phase advancement and an increased number of spikes per cycle. Note that the discharges are confined mostly to the rising phase of the oscillation, similar to the experimental observation (Fig. 4). This is because during the rising phase, the I_{KS} is slowly activated and reduces the excitability of the cell for the rest of the cycle. The current scale applies to both I_{KS} and I_{soma} .

current injection dramatically increased the amplitude of intracellular theta when the membrane was depolarized to more than -45 mV ($n = 6$; Fig. 7). Similar wide spikes could be evoked by depolarizing current steps (Figs. 6B, 7B). In contrast to somatic recordings, dendritic recordings often showed large variability in the amplitude of theta-related voltage fluctuations. Occasionally, large amplitude waves emerged from the low amplitude background without any noticeable change in the extracellular theta even without current-induced depolarization of the membrane (Fig. 8A, B). These large amplitude events and the associated fast (Na^+) spikes occurred on the positive phase of the field theta in the pyramidal layer (Fig. 8A, B). Such large amplitude intradendritic theta episodes could also be evoked by low-intensity tetanic stimulation of the commissural pathway (Fig. 8C). The stimulus

train evoked a brief afterdischarge followed by an 0.5-to-2.0-s episode of large amplitude rhythmic waves at theta frequency.

In three experiments we used QX 314 in the recording pipette to block the fast Na^+ spikes (Figs. 8B and 9). With steady depolarization, the cycle-by-cycle amplitude fluctuation of the membrane potential became uneven and large-amplitude, wide spikes alternated with more regularly sized cyclic events. The large spikes, putative high-threshold calcium spikes (Wong et al., 1979), occurred irregularly between -50 mV and -45 mV membrane potential but became rhythmic in the theta frequency range when the membrane was further depolarized.

Cross-correlating the extracellular theta with intradendritic theta revealed that the depolarizing phase of the intradendritic oscillation coincided with the positive phase of the field theta in the pyramidal cell layer (Fig. 10). In this context, it is important to emphasize that it is the negative peak of the field theta activity in the pyramidal layer that corresponds to somatic depolarization (Fig. 2B) and to the maximum probability of population discharge of pyramidal cells (Fig. 10; Buzsáki et al., 1983; Soltész and Deschênes, 1993; Ylinen et al., 1995b; Skaggs et al., 1996).

Voltage-dependent (Intrinsic) Theta Oscillation in Dendrites

Although the network-embedded pyramidal cells are under a strong control of their afferent inputs, as evidenced by the relationship between intracellular membrane potential changes and the extracellularly recorded field, dendrites could also sustain an intrinsic oscillation. Strong depolarization, even in the absence of extracellularly recorded theta activity, could induce a highly regular rhythm (Fig. 11). Moreover, the frequency of the dendritic oscillatory rhythm could be increased with further depolarization (Fig. 11). Similar observations were made in four additional dendritic recording experiments. These findings indicated that intrinsic properties of pyramidal cell dendrites may actively contribute to the theta pattern.

Modeling of Spike Phase Precession by Theta Oscillations in Soma and Dendrite

To test our hypothesis on the contributions of active dendritic mechanisms to the advancement of action potentials, we simulated the computational model with an increased g_{NaP} (0.1 instead of 0.05) and a reduced g_{KS} (0.9 instead of 1.4), so that the dendritic compartment became powerfully excitable. With such modest change of parameters, the model displayed repetitive rhythmic bursting (<15 Hz, at two to five spikes/burst), in response to constant current injection (data not shown). An additional change, compared to the model shown in Figure 5, is that the dendrite was rhythmically excited, in accord with our intradendritic observations. To mimic the passage of a rat across the place field, let us suppose that the excitatory drive to the neuron's dendrite is gradually increased as the rat enters and moves across the place field. In simulations, we considered a dendritic input current consisting of a constant and a sinusoidal component, $I_{\text{dendrite}} = A + B \sin(2\pi f t)$, and we investigated how the timing of spikes with respect to the somatic theta input was

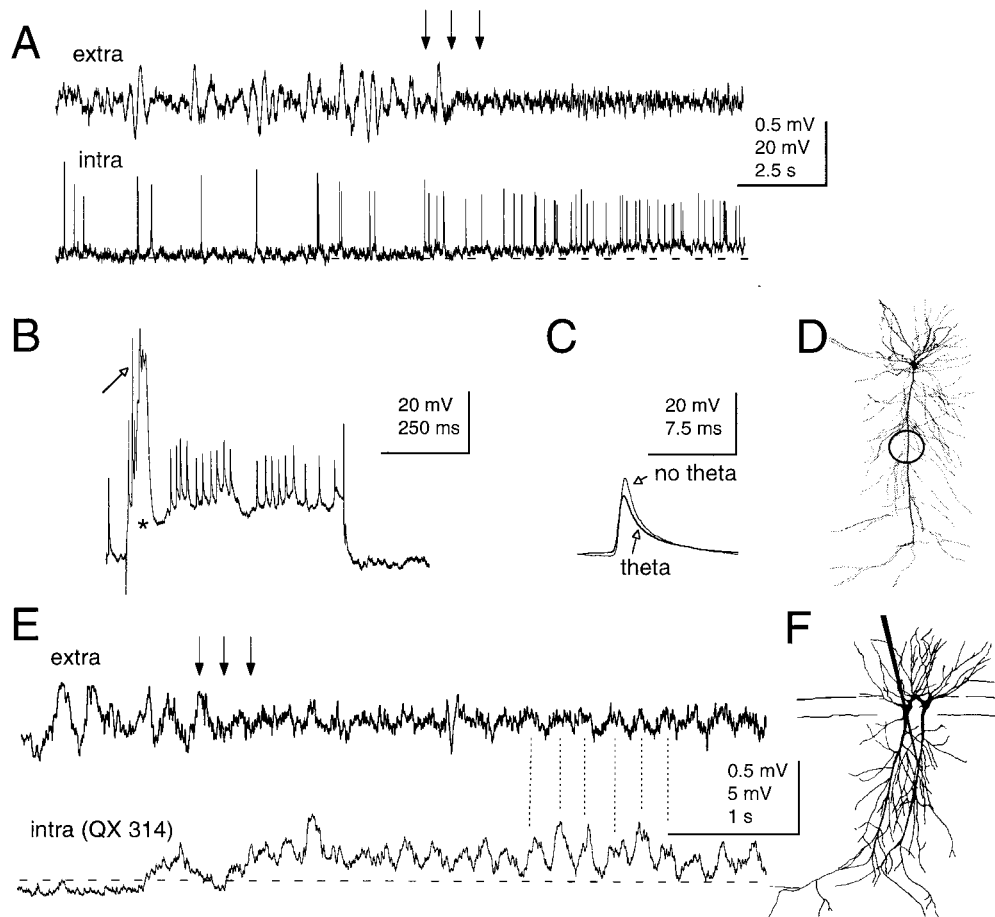


FIGURE 6. Theta is associated with dendritic depolarization. A: Simultaneous recording of extracellular EEG activity in the CA1 pyramidal layer (extra) and intradendritic activity (intra) of a pyramidal cell. Note steady depolarization of the pyramidal cell membrane at the onset of spontaneous theta activity (arrows). Dotted line represents -67 mV. Note also decreased amplitude of action potentials during theta. **B:** Response of the dendrite to 0.8 nA current injection. Note large amplitude fast spike (arrow) and slow spike (asterisk). **C:** Averaged action potentials during no theta and theta

periods. Note slow spike decay and absence of spike afterhyperpolarization. **D:** Estimated location of dendritic penetration (circle). **E:** Similar experiment to A but the recording pipette contained QX 314 to block Na^+ spikes (20 mM). Dotted line represents -62 mV. Arrows indicate tail pinch. **F:** Estimated position of dendritic impalement for neuron shown in E. Drawing tube reconstruction of the biocytin filled cell and the recording pipette track. Another neuron was also recorded from the soma in this animal (shown in Figure 2B).

varied when the parameters A and B were increased. For the sake of simplicity, we assumed that $I_{dendrite}$ had a same oscillation frequency ($f = 7$ Hz) as I_{soma} and that the two inputs were 180 degrees out of phase, mimicking the observation that somatic hyperpolarization is phase-locked with dendritic depolarization.

With increasing drive to the dendrite, progressively larger phase-advancement of the action potentials, relative to the somatic theta phase, was observed (Fig. 12). Unlike the model without intrinsic burst firing (Fig. 5), now both the onset and offset of bursts shifted gradually to earlier “theta” phase. Moreover, the phase shift could be more than 180 degrees because, when strongly driven by the dendritic input, the model neuron was able to initiate bursts of spikes at the rising phase (rather than the peak) of $I_{dendrite}$. Spikes could be triggered at all phases of the theta cycle. In addition to large phase-shifts, double bursts rising from different polarization levels were also observed (Fig. 12f). This occurred when tonic depolarization (parameter A) was large but

the amplitude of modulation (parameter B) was relatively small, so that temporal modulation of the dendritic input is not strong enough to “clamp” the cell’s firing to the peak of the dendritic input. These double bursts are reminiscent of the double-discharge pattern observed in a portion of pyramidal cells during spatial behavior (see units 12, 29, 32 and 40 of Figure 7 in Skaggs et al., 1996). In summary, the computational results, in corroboration with the experimental data, suggest that active dendritic responsiveness plays an important role in the timing of the action potentials.

DISCUSSION

The main findings of the present experiments are that 1) perisomatic inhibition of pyramidal neurons is coupled with

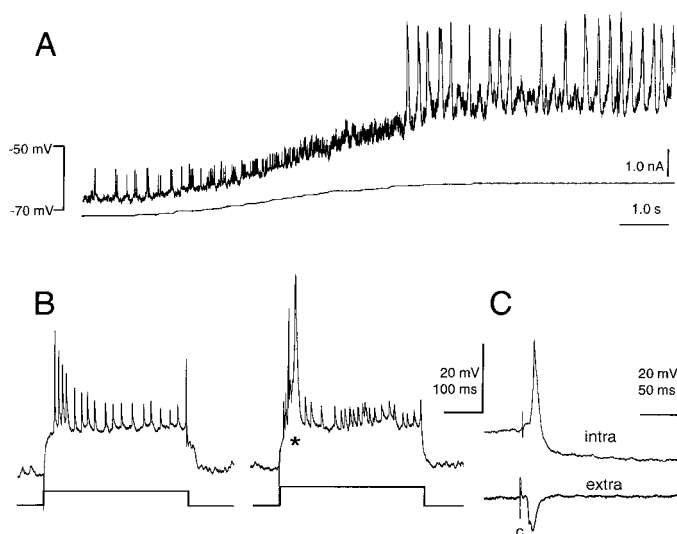


FIGURE 7. Current-induced high-threshold calcium spike oscillation in a pyramidal cell dendrite. Impalement was made 370 μm below the pyramidal cell layer. **A:** Holding potential was manually shifted to progressively more depolarized levels by intradendritic current injection (lower trace). Note partial blockade of fast (Na^+) spikes and rhythmic occurrence of large amplitude wide spikes. **B:** Responses of the dendrite to 0.6 and 0.8 nA current steps. Note decrementing amplitude spikes (left) and large amplitude slow spike (asterisk). **C:** Evoked dendritic response by commissural stimulation (c; intra). The field evoked response after the recording pipette was withdrawn from the dendrite is also shown (extra).

depolarization of the distal apical dendrites during theta activity, 2) theta is associated with a large decrease in the input resistance of the cell, 3) the degree of dendritic depolarization is reflected by the timing of action potentials within the theta cycle, 4) dendrites can actively support a high threshold rhythm in the theta frequency band and 5) theta oscillation of the somatic and dendritic membrane produces a systematic phase advancement of action potentials.

Somatic and Dendritic Generators of Hippocampal Theta Activity

Ample evidence supports the hypothesis (Buzsáki et al., 1983) that part of theta activity derives from the rhythmic hyperpolarization of the pyramidal cell somata (Fox, 1989; Leung and Yim, 1991; Soltész and Deschénes, 1993; Cobb et al., 1995; Ylinen et al., 1995b; Toth et al., 1997; but see also Nuñez et al., 1987, 1990; Konopacki et al., 1992). At the onset of hippocampal theta rhythm the somatic membrane displayed oscillatory waves in the hyperpolarizing direction (see also Figure 2 of Konopacki et al., 1992). This "somatic" theta is mainly due to the rhythmic discharge of basket cells and the IPSPs are mediated by GABA_A synapses (Cobb et al., 1995; Ylinen et al., 1995b; Toth et al., 1997). At the same time, dendrites are depolarized (see below). At the onset of the theta rhythm, the input resistance of the soma decreased considerably. Such a dramatic shunting of the somatic region, due to the coherent activity of basket cells, may effectively prevent the passive spread of dendro-somatic depolarization and

attenuate the active backpropagation of action potentials from the soma to the dendrites (Spruston et al., 1995; Buzsáki et al., 1996; Tsubokawa and Ross, 1996). Indeed, we found that the mean and variability of spike amplitude in dendritic recordings were less during theta activity than in its absence (see also Kamondi et al., in press). The shunting effect of inhibition on the somatic spike amplitude was demonstrated by activation of feed-forward inhibition by the commissural input. The reduction in spike amplitude was much larger than what might be expected from the level of hyperpolarization; thus it is likely that shunting the somatic membrane played an important role in the amplitude decrease of somatic action potentials.

In addition to the perisomatic dipole, previous depth profile measurements of theta waves already suggested the presence of other theta dipoles in the CA1 region (Winson, 1974; Buzsáki et al., 1983, 1986; Brankack et al., 1993). In the awake rat, theta activity reverses gradually from the pyramidal layer to the hippocampal fissure. The largest amplitude theta occurs around the hippocampal fissure (sometimes this is erroneously referred to as "dentate" theta). The large current sink in stratum lacunosum-moleculare suggests that at the time of the somatic outward current (source) the distal apical dendrites are depolarized. This large theta dipole is likely produced by the perforant path input because it was abolished by bilateral removal of the entorhinal cortex and because layer III pyramidal cells of the entorhinal cortex discharge phase-locked to the theta rhythm (Mitchell and Ranck, 1980; Alonso and Garcia-Austt, 1987; Ylinen et al., 1995b; Chrobak and Buzsáki, 1998).

Similar to the current-source density analysis, the intracellular experiments indicated that somatic hyperpolarization and dendritic depolarization overlap in time. Although simultaneous recordings from the soma and dendrite of the same pyramidal cell were not attempted, the sequential recordings clearly indicated that the positive portion of the extracellular theta in the pyramidal layer corresponded to the hyperpolarization phase of intrasomatic theta and to a minimum of spike discharge probability of pyramidal cells (Buzsáki et al., 1983; Fox, 1989; Leung and Yim, 1992; Ylinen et al., 1995). This same phase of extracellular theta, on the other hand, correlated with intradendritic depolarization, indicating that dendritic depolarization and somatic hyperpolarization occur at the same time. The charges carried by the respective ions (Na^+ and Cl^-) are responsible for the outward current in the somatic region (active source) and the inward current in the distal dendrites (active sink). Because the charges from these respective synaptic regions move in the same direction in the extracellular space, they cooperatively produce the large amplitude field theta. In addition to these two major dipoles, efferents of all intrahippocampal and extrahippocampal cell groups, phase-locked to theta waves, may contribute to the rhythmic field pattern (Buzsáki et al., 1986; Brankack et al., 1993). The systematic phase-shifts of these various dipoles are responsible for the unique voltage-vs.-depth profile of theta activity in the behaving animal (Winson, 1974; Bland et al., 1975; Buzsáki et al., 1983; Leung, 1984; Buzsáki et al., 1986; Lopes da Silva et al., 1990; Brankack et al., 1993).

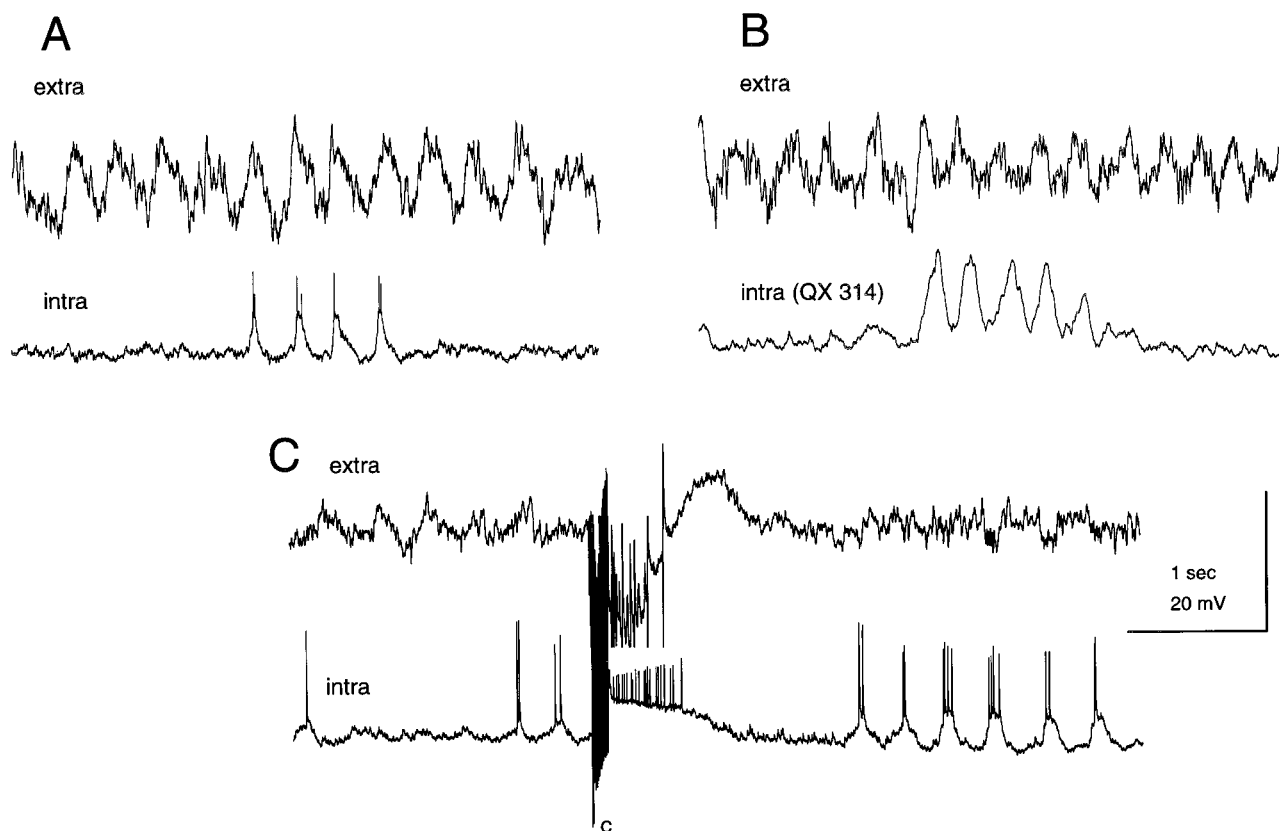


FIGURE 8. Transient large amplitude theta rhythm episodes in dendrites. A, B: Spontaneous large amplitude events in distal dendrites (intra) without any noticeable change in the extracellular theta (extra). The electrode in B contained QX 314. C: Large amplitude intradendritic theta episodes could also be evoked by low

intensity tetanic stimulation of the commissural pathway (c; 100 Hz, 200 ms). The tetanus evoked a brief afterdischarge followed by an 0.5-to-2.0-s episode of large amplitude rhythmic waves and bursts of fast spikes at theta frequency.

The interplay between somatic inhibition and dendritic excitation has important consequences for the output of the pyramidal neurons. First, despite rhythmic intradendritic depolarizations, the action potential generation of the pyramidal cells can be prevented altogether. Various estimates indicate that during a given cycle of theta activity in the behaving rat only a very small percentage of all pyramidal cells discharge (Fox et al., 1986; Buzsáki, 1989; Thompson and Best, 1989; Skaggs et al., 1996). The reason is that perisomatic inhibition and shunting keep the membrane potential of the soma and axon initial segment just below spike threshold. Second, assuming a stochastic input, pyramidal cells can be discharged with the least amount of excitation during the negative phase of field theta in the pyramidal layer (i.e., when the soma is least hyperpolarized). This explains why the peak discharge of the population is phase-locked to the negative peak of the field theta in the pyramidal layer when discharges of multiple pyramidal cells are cross-correlated with the field theta for long time periods (Buzsáki et al., 1983; Fox et al., 1986; Skaggs et al., 1996). Finally, strong depolarization of the dendritic membrane may overcome the somatic inhibition at any time, provided that the depolarizing force is sufficient to overcome perisomatic inhibition. Such effective depolarization may be brought about by converging activity of perforant path inputs and

associational afferents on the same pyramidal cell (Buzsáki et al., 1995). Activation of Ca^{2+} and/or suppression of K^+ channels in the more proximal dendrites by the Schaffer collaterals may boost the effectiveness of the perforant path-mediated EPSPs on the apical tuft and bring pyramidal cells to spike threshold. The occasional large amplitude depolarizing episodes observed in our experiments provide support for these possibilities.

Although direct evidence is available for the notion that somatic inhibition during theta activity in the intact rat is brought about by basket cells (Ylinen et al., 1995b), the exact pacemaker inputs to the basket cells have yet to be discovered. GABAergic neurons of the medial septum selectively target hippocampal interneurons (Freund and Antal, 1988; Toth et al., 1997). However, it is notable that the dendritic morphology of basket cells permits that the same afferents which innervate pyramidal cells also contact basket cells. Basket and chandelier cells are innervated by the entorhinal input (Kiss et al., 1996) and they can be discharged monosynaptically by perforant path stimulation (Buzsáki and Eidelberg, 1982). Chandelier cells may be particularly important in this monosynaptic event since their apical dendrites have very few branches in the stratum radiatum but a large apical tuft in the stratum lacunosum-moleculare (Li et al., 1992; Buhl et al., 1994). Stimulation of the entorhinal afferents

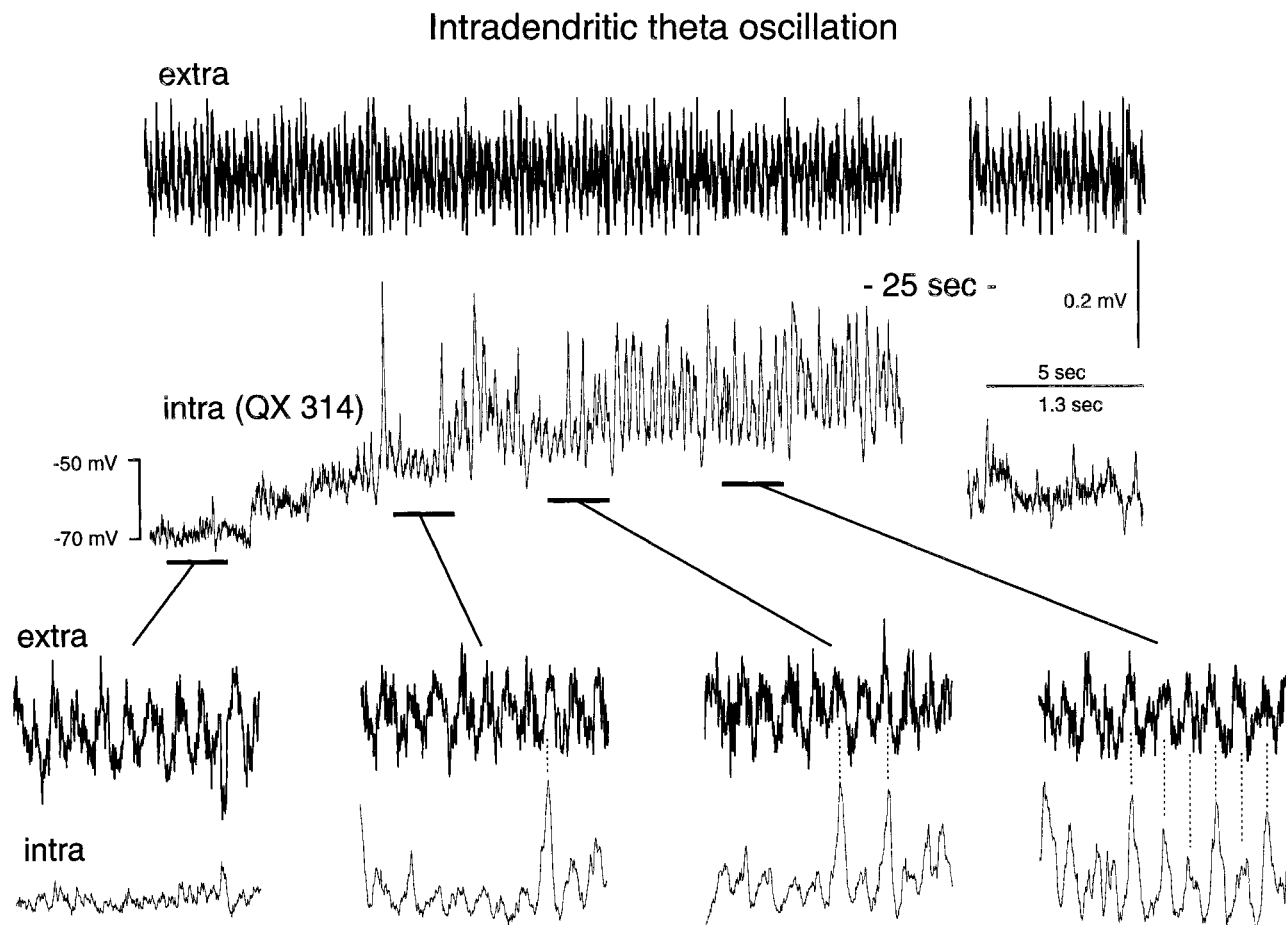


FIGURE 9. Voltage-dependence of theta oscillation in a pyramidal cell dendrite. Continuous recording of extracellular (extra) and intradendritic (intra) activity in a CA1 pyramidal cell. Holding potential was manually shifted to progressively more depolarized levels by intradendritic current injection (0 to 0.8 nA). The marked epochs (horizontal bars) are shown at faster speed in the bottom

records. The recording electrode also contained QX 314 to block Na^+ spikes (20 mM). Note large increase of intradendritic theta oscillation amplitude upon depolarization. The relationship of the putative high threshold calcium spikes to the phase of extracellular theta in the CA1 pyramidal layer is indicated by dotted lines. Same pyramidal cell as shown in Figures 6E and F.

evokes IPSPs at the same latency as the monosynaptic discharge of basket/chandelier neurons (Colbert and Levy, 1992; Soltész and Deschénes, 1993; Buzsáki et al., 1995). Attenuation of this feed-forward inhibition can reveal monosynaptic excitation of pyramidal cells by the perforant path (Yeckel and Berger, 1990; Colbert and Levy, 1992; Buzsáki et al., 1995). Given the cyclic inhibition and excitation of these interneurons by the medial septum and the entorhinal input, respectively, changes in their discharge rate during the theta waves should have important consequences on the firing pattern of their target principal cells.

Voltage-Dependent Theta Oscillation in Dendrites

When dendritic depolarization was sufficiently strong, the resonant property of the membrane gave way to a self-sustained oscillation in the theta frequency range, even in the absence of network-driven theta activity. Intrinsic, voltage-dependent slow oscillations and theta frequency resonance have been observed in somatic recordings of hippocampal pyramidal cells (Leung and Yim, 1991; Leung and Yu, 1998), thalamocortical neurons

(Steriade et al., 1993; Pedroarena and Llinas, 1997) and stellate cells of the entorhinal cortex (Alonso and Llinas, 1989) and layer V-VI pyramidal cells of the neocortex (Silva et al., 1991). In stellate cells, the main driving force of the oscillation is a persistent Na^+ current (Alonso and Llinas, 1989), whereas another depolarizing current (I_h), in conjunction with the low threshold Ca^{2+} current (I_T), is responsible for the maintenance of the cellular rhythm in thalamic neurons (Bal et al., 1995). Although the exact ionic mechanisms underlying intradendritic theta frequency oscillation have yet to be disclosed, QX 314-resistant channels are likely involved since intrinsic theta oscillation persisted after intradendritic injection of the drug.

The voltage-dependent oscillatory property of pyramidal cells has important implications for their network activity, including the phase precession of spike burst patterns during spatial behavior (see below). However, it remains to be demonstrated whether coactivation of synaptic inputs in the behaving rat can provide a sufficient degree of depolarization for the local induction of calcium spikes underlying the rhythmic events. Initiation of

calcium spikes in distal apical dendrites of layer V pyramidal cells by synaptic activation requires coactivation of AMPA- and NMDA-type glutamate receptors (Schiller et al., 1997). Although large calcium spikes have been observed in connection with hippocampal sharp wave bursts (Kamondi et al., 1998), their rare presence during theta may be explained by the NMDA-receptor blockade of urethane. As discussed earlier, the theta dipole in the stratum lacunosum-moleculare is strongly attenuated by both urethane and ketamine (Soltész and Deschènes, 1993; Ylinen et al., 1995b). Nevertheless, if the synaptic actions are considerably stronger in the drug-free animal, the present findings raise the possibility that input synapses of place cells could be modified by the dendritic calcium events.

Timing of Action Potentials During Theta Waves

In the experiments with sinusoid current patterns, the first spike as well as the peak of the spike density progressed to an earlier phase of theta with increasing levels of somatic depolarization. Action potentials on the decaying phase of theta occurred rarely. Computer simulation indicated that dendritic depolarization alone was not sufficient to replicate the magnitude of the empirically observed phase advancement. Action potentials occurred symmetrically with respect to the peak of the input current

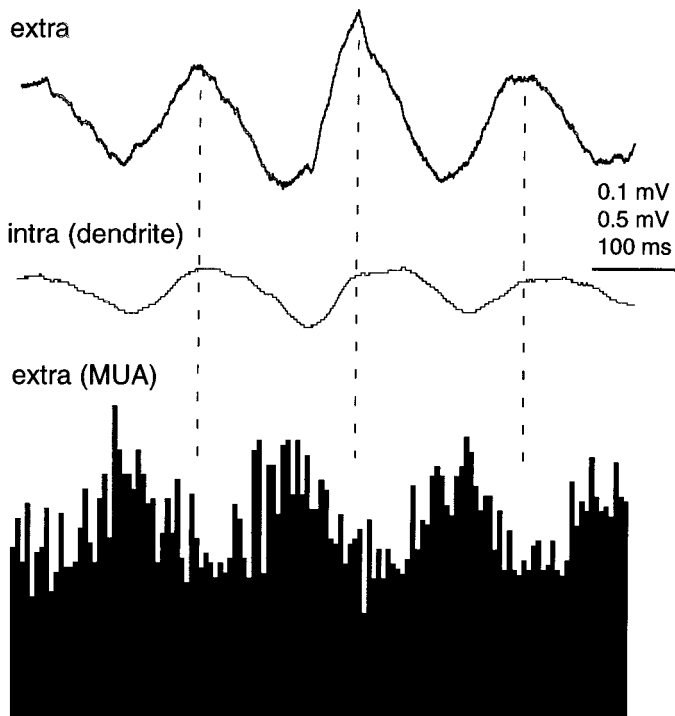


FIGURE 10. Event-related averages of extracellular theta, intradendritic voltage and multiple unit activity (MUA) of pyramidal cells. Reference trigger: Zero crossings of extracellular theta activity. Note that the positive peaks of the extracellular theta waves recorded in the CA1 pyramidal layer (dashed lines) correspond to the depolarizing phase of the intradendritic potential (intra, dendrite) and decreased spiking of pyramidal cells (n = 50 reference events).

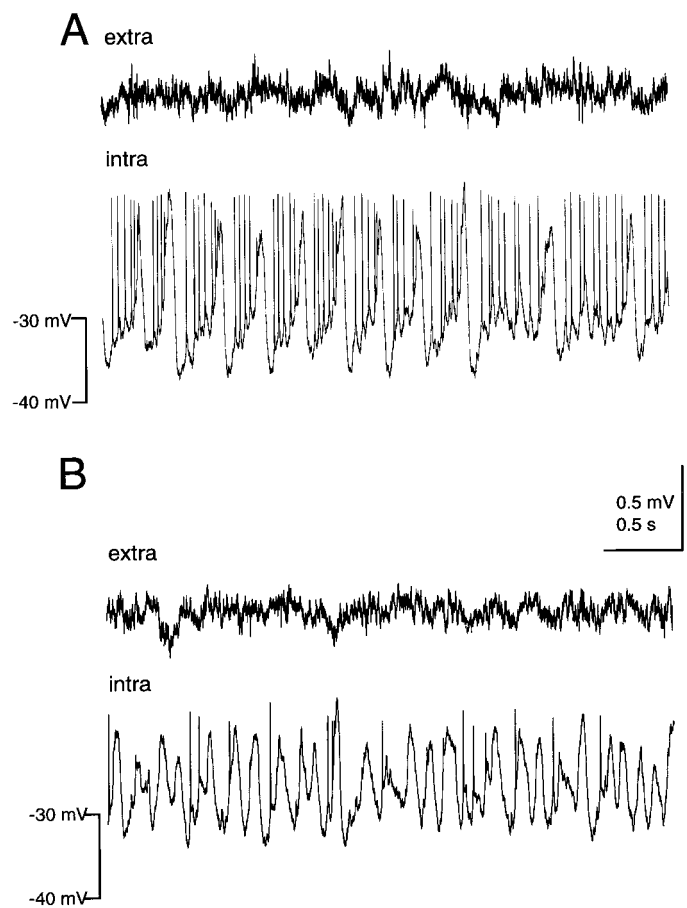


FIGURE 11. Depolarization-induced rhythmic oscillation of the dendritic membrane in the absence of background theta activity. (Impalement 180 μm below pyramidal layer.) A: Simultaneous recording of extracellular EEG activity in the CA1 pyramidal layer (extra) and intradendritic activity of the pyramidal cell (intra). The dendrite was depolarized by constant current injection (0.8 nA). Note rhythmic occurrence of putative calcium spikes and associated fast spikes at approximately 4 Hz. B: Further depolarization (1.0 nA) increased the frequency of membrane oscillation to 7–8 Hz. Note partial or full blockade of fast spikes.

cycle. The addition of the slow K⁺ current I_{KS} and Na⁺ current I_{NaP} , however, induced asymmetrical discharge during input cycle, similar to that observed during sinus current injection and naturally occurring theta. It is possible that similar currents may be responsible for the asymmetric discharge of the pyramidal cells with respect to the theta cycle in the intact brain as well. Because intracellular depolarization is a consequence of the spatiotemporal convergence of excitatory afferents on the dendrites, the phase position of the action potential on the theta cycle may faithfully reflect the neuron's transformation of the input to the output (spike). Therefore, phase advancement of the action potentials and increased number of action potentials per theta cycle observed in the behaving rat may be taken as an indication of progressively stronger dendritic depolarization of the recorded cell. These experiments therefore support the view that phase deviation from average behavior is the relevant neural information (cf., Buzsáki and Chrobak, 1995; Hopfield, 1995).

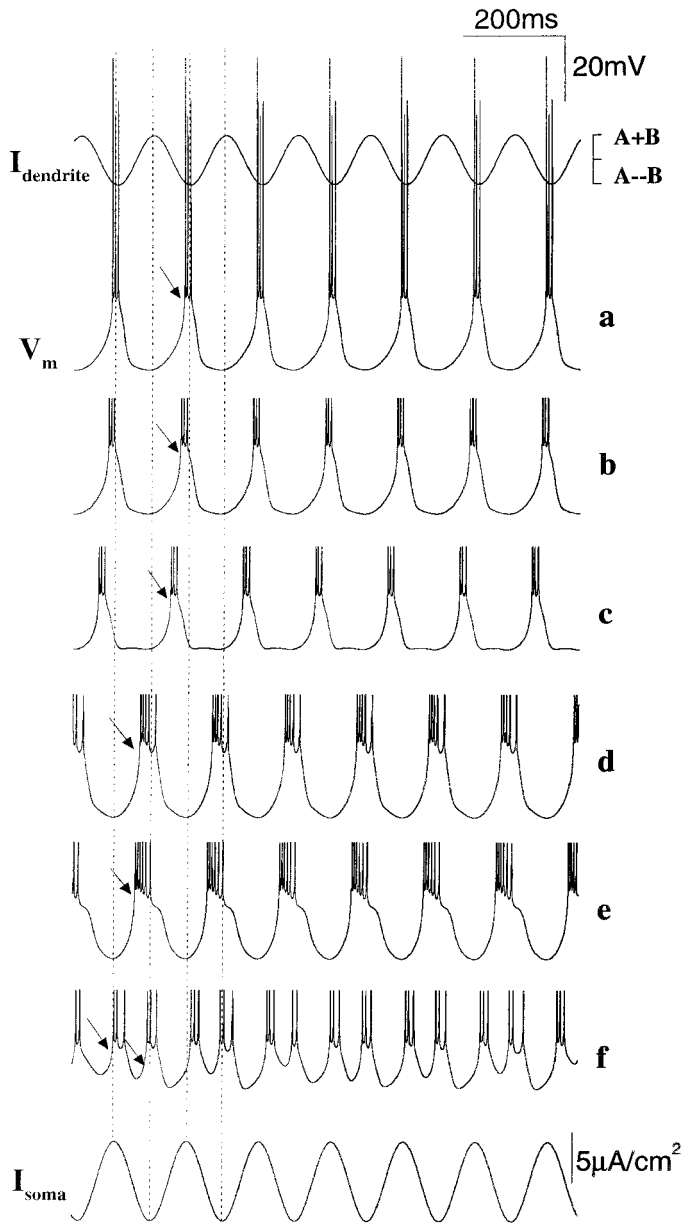


FIGURE 12. Phase precession of action potentials in a model neuron with intrinsic rhythmic bursting ($g_{NaP} = 0.1$ and $g_{Ks} = 0.7$; other parameters are the same as in Figure 6). Bottom panel: Sinusoidal current applied to the soma at 7 Hz. Dendritic injected current $I_{dendrite} = A + B \sin(2\pi ft)$ is schematically illustrated in the top panel; values of A and B vary from panel to panel. $I_{dendrite}$ is 180 degrees out-of-phase with I_{soma} . With small $I_{dendrite}$ (panel a), the soma fires at the peak of I_{soma} (= trough of $I_{dendrite}$). Stronger $I_{dendrite}$ produces gradual phase advancement of the burst discharges up to 360 degrees. The first spike of the burst is marked by arrows. "Double" phase advancement shown in f has also been observed empirically (Skaggs et al., 1996). The parameters of A and B, and the phase shifts of the burst onset, center and offset (in degrees) are as follows: (a) A = 0.8, B = 0.16, onset = -20, center = -6.5, offset = +8; (b) A = 1.0, B = 0.2, onset = -36, center = -23, offset = -9; (c) A = 1.5, B = 0.3, onset = -85, center = -70.7, offset = -57; (d) A = 1.8, B = 2.2, onset = -240, center = -210, offset = -154; (e) A = 3.5, B = 2.5, onset = -258, center = -224, offset = -182; (f) A = 4, B = 1, onset = -350, center = -238, offset = -150.

Phase Precession of Pyramidal Cells During the Theta Cycle

To date, the most convincing experimental support for the "phase coding" of information discussed above is the phenomenon of spike phase precession. O'Keefe and Recce (1993) have discovered that the action potentials of "place-coding" pyramidal cells undergo a systematic phase precession while the rat crosses the field of the recorded unit. Importantly, the phase of theta at which the cell fired was a better predictor of the animal's position than the firing rate of the neuron (see also Skaggs et al., 1996). Several computational models attempted to explain this important physiological phenomenon (O'Keefe and Recce, 1993; Lisman and Idiart, 1995; Tsodyks et al., 1996; Wallenstein and Hasselmo, 1997). Phase precession of spikes in the behaving animal has the following main features: 1) increased number of action potentials as the rat moves towards the center of the field and decreasing number of spikes as the animal leaves the center; 2) peak firing rate in the center of the field; 3) the onset of spikes moves to progressively earlier phases of the extracellularly recorded theta cycle, sometimes up to 360 degrees; 4) consequently, spikes can occur at all phases of the theta cycle.

Our observations on dendritic-somatic domain competition may shed light on the mechanism of phase advancement of action potentials. Several similarities between our somatic depolarization experiment and model and the phase precession of spike activity in the behaving animal are worth mentioning. First, stronger depolarization induced both larger phase precession and more action potentials. In the middle of the field, place cells fire more action potentials than at the periphery, presumably because the cell is more strongly excited in the center of the field. Second, weakly active cells show less phase precession than strongly active ones (Skaggs et al., 1996), again in accord with our observations. Third, the amplitude of the extracellular place units decreases as the rat moves towards the center of the field (M. A. Wilson, personal communication). This may happen because spikes emanate from progressively more depolarized membrane potential levels as the rat approaches the middle of the field. Some place cells show progressive phase advancement and reduction of phase shift as the rat approaches and exits the center of the field, respectively (O'Keefe and Recce, 1993). Our intrasomatic observations with sinus current and tonic depolarization along with the associated model can fully explain this behavior. However, these findings alone fail to account for the >180-degree phase precession observed in most place cells (O'Keefe and Recce, 1993; Skaggs et al., 1996). Furthermore, discharge patterns cannot always be described in terms of a linear phase advance and many place cells show quite complex dynamics (Skaggs et al., 1996). Finally, in the middle of the field, the firing of many place cells spans the entire theta cycle. This was not the case with tonic depolarization at the soma.

In their interpretation of the progressive phase shift of place cells, O'Keefe and Recce (1993) hypothesized the presence of two rhythm generators oscillating at slightly different frequencies. According to their hypothesis, one of these oscillators increases slightly over the other as the rat approaches the middle of the field.

The origin of the oscillators was not explored, however. One possibility is that the frequency increase occurs in the entorhinal input to the hippocampus. Such generalized frequency difference between the entorhinal and direct septal afferents is unlikely, however, given their common pacemaker input, the septal area. Another hypothesis was put forward by Skaggs et al. (1996). Because phase precession was also observed in granule cells, these authors suggested that phase-advancement is "passively" conveyed to the CA1 pyramidal cells by the Schaffer collaterals of CA3 pyramidal neurons.

Our intradendritic findings offer an alternative explanation of spike precession. Dendritic recordings revealed a depolarizing membrane rhythm whose phase was opposite to the theta fluctuation observed in the soma. Large amplitude spontaneous depolarizing rhythms and associated spiking were also observed occasionally in distal dendrites, suggesting that convergence of presynaptic activity to a particular dendritic segment can be very effective. We hypothesize that in the awake, drug-free rat the convergent excitation of pyramidal cell dendrites by the entorhinal and, possibly, CA3 collaterals can be sufficiently strong in the middle of the neuron's place field to induce large amplitude dendritic EPSPs and bursts of action potentials. This hypothesis was tested in the pyramidal cell model with bursting properties. Mimicking the experiment, out-of-phase theta oscillation was fed into the soma and dendrite of the model neuron. Depending on the modulation depth of the theta rhythm and the amount of steady depolarization applied to the dendritic compartment, phase-shifts occurred. The magnitude of the phase shift was commensurate with the amplitude of the dendritic theta modulation and the magnitude of the steady depolarization. The first spike of the burst could advance up to 360 degrees. As a result, spikes occurred at all phases of the theta cycle. The intradendritic experiments and the associated model therefore indicate that rhythmic dendritic excitation, coupled with somatic inhibition, can account for the major aspects of the spike phase precession observed in the behaving animal.

A further complexity that may be added to the above picture is that strong intradendritic depolarization could induce an intrinsic membrane oscillation. The frequency of the induced rhythm was voltage-dependent and could be faster than the frequency of field theta. If similar strong depolarization can occur in the pyramidal cell dendrites of the awake drug-free rat then a more complex action potential-theta phase relationship is expected than what can be induced by out-of-phase dendritic and somatic oscillatory patterns.

Because our intracellular recordings were carried out in the anesthetized rat, the objection can be made that the explanation we have provided for the spike phase advancement of place cells may not hold in the drug-free animal. However, the conditions under which pyramidal cells were tested are expected to be very similar in the behaving rat. Dendritic depolarization is needed for discharging pyramidal cells. Theta modulation is present in both dendrites and soma of these neurons during spatial behavior. The findings therefore suggest that these two conditions are sufficient to induce phase-advancement and burst discharge of pyramidal cells. It remains to be disclosed what additional mechanisms shape

the firing patterns of pyramidal neurons to produce more the complex dynamics observed in some place cells.

Acknowledgments

László Acsády and Anita Kamondi were visiting scholars at Rutgers University. We thank Drs. A. Bragin and M. Penttonen for helping with some of the experiments, J. Csicsvari, H. Hirase, C. King, and M. Recce for their comments on the manuscript, Helen Olivera for processing part of the histological material, A. Alonso for communicating his voltage-clamp data, and B. Craft for his participation in model simulations. This work was supported by NIH (NS34994, MH54671, MH53717), the Alfred P. Sloan Foundation, the Human Frontier Science Program, the Soros Foundation, and the Whitehall Foundation.

REFERENCES

- Alonso A, Garcia-Austt E. Neuronal sources of theta rhythm in the entorhinal cortex of the rat. I. Laminar distribution of theta field potentials. *Exp Brain Res* 1987;67:493–501.
- Alonso A, Llinas RR. Subthreshold Na^+ -dependent theta-like rhythmicity in stellate cells of entorhinal cortex layer II. *Nature* 1989;342:175–177.
- Andrade R. Blockade of neurotransmitter-activated K^+ conductance by QX 314 in the rat hippocampus. *Eur J Pharmacol* 1991;199:259–262.
- Andreasen M, Lambert JDC. Regenerative properties of pyramidal cell dendrites in area CA1 of the rat hippocampus. *J Physiol (Lond)* 1995;483:421–441.
- Artemenko DP. Role of hippocampal neurons in theta-wave generation. *Neurophysiologia* 1972;4:409–415.
- Bal T, von Krosigk M, McCormick DA. Synaptic and membrane mechanisms underlying synchronized oscillations in the ferret lateral geniculate nucleus in vitro. *J Physiol (Lond)* 1995;483:641–663.
- Bland BH. Physiology and pharmacology of hippocampal formation theta rhythms. *Prog Neurobiol* 1986;26:1–54.
- Bland BH, Andersen P, Ganes T. Two generators of hippocampal theta activity in rabbits. *Exp Brain Res* 1975;94:199–218.
- Boeijinga PH, Lopes da Silva FH. Modulations of EEG activity in the entorhinal cortex and forebrain olfactory areas during odour sampling. *Brain Res* 1989;478:257–268.
- Bragin A, Jando G, Nadasdy Z, Hetke J, Wise K, Buzsáki G. Gamma frequency (40–100 Hz) patterns in the hippocampus of the behaving rat. *J Neurosci* 1995;15:47–60.
- Brankack J, Stewart M, Fox SE. Current source density analysis of the hippocampal theta rhythm: associated sustained potentials and candidate synaptic generators. *Brain Res* 1993;615:310–327.
- Buhl EH, Han ZS, Lorinczi Z, Stezhka VV, Karnup SV, Somogyi P. Physiological properties of anatomically identified axo-axonic cells in the rat hippocampus. *J Neurophysiol* 1994;71:1289–1307.
- Buzsáki G, Chrobak JJ. Temporal structure in spatially organized neuronal ensembles: A role for interneuronal networks. *Curr Opin Neurobiol* 1995;5:504–510.
- Buzsáki G, Eidelberg E. Direct afferent excitation and long-term potentiation of hippocampal interneurons. *J Neurophysiol* 1982;48:597–607.
- Buzsáki G, Leung L, Vanderwolf CH. Cellular bases of hippocampal EEG in the behaving rat. *Brain Res Rev* 1983;6:139–171.

- Buzsáki G, Czopf J, Kondakor I, Kellenyi L. Laminar distribution of hippocampal rhythmic slow activity (RSA) in the behaving rat: Current source density analysis, effects of urethane and atropine. *Brain Res* 1986;365:125-137.
- Buzsáki G, Bragin A, Chrobak JJ, Nadasdy Z, Sik A, Hsu M, Ylinen A. Oscillatory and intermittent synchrony in the hippocampus: Relevance to memory trace formation. In: Buzsáki G, Llinás R, Singer W, Bethoz A, Christen Y, eds. *Temporal coding in the brain*. Berlin: Springer-Verlag, 1994:145-172.
- Buzsáki G, Ylinen A, Penttonen M, Bragin A, Nadasdy Z, Chrobak JJ. Possible physiological role of the perforant path-CA1 projection. *Hippocampus* 1995;5:141-146.
- Buzsáki G, Penttonen M, Nadasdy Z, Bragin A. Pattern and inhibition-dependent invasion of pyramidal cell dendrites by fast spikes in the hippocampus in vivo. *Proc Natl Acad Sci USA* 1996;93:9921-9925.
- Chrobak JJ, Buzsáki G. Gamma oscillation in the entorhinal-hippocampal axis of the freely-behaving rat. *J Neurosci* 1997;18:388-398.
- Cobb SR, Buhl EH, Halasy K, Paulsen O, Somogyi P. Synchronization of neuronal activity in hippocampus by individual GABAergic interneurons. *Nature* 1995;378:75-98.
- Colbert CM, Levy WB. Electrophysiological and pharmacological characterization of perforant path synapses in CA1: Mediation by glutamate receptors. *J Neurophysiol* 1992;68:1-8.
- Connors BW, Prince DA. Effects of the local anesthetic QX 314 on the membrane properties of hippocampal pyramidal neurons. *J Pharmacol Exp Ther* 1982;220:476-481.
- Fox SE. Membrane potential and impedance changes in hippocampal pyramidal cells during theta rhythm. *Exp Brain Res* 1989;77:283-294.
- Fox SE, Wolfson S, Ranck JB Jr. Hippocampal theta rhythm and the firing of neurons in walking and urethane anesthetized rats. *Exp Brain Res* 1986;62:495-508.
- Freund TF, Antal M. GABA-containing neurons in the septum control inhibitory interneurons in the hippocampus. *Nature* 1988;336:170-173.
- Fujita Y, Sato T. Intracellular records from hippocampal pyramidal cells in rabbit during theta rhythm activity. *J Neurophysiol* 1964;27:1011-1025.
- Galue A, Alonso A. Properties of the persistent Na current generating subthreshold oscillations in entorhinal cortex (EC) layer II neurons. *Soc Neurosci Abstr* 1996;22:34.2.
- Gray CM, Koenig P, Engel AK, Singer W. Stimulus-specific neuronal oscillations in cat visual cortex exhibit inter-columnar synchronization which reflects global stimulus properties. *Nature* 1989;338:334-337.
- Hoffman DA, Magee JC, Colbert CM, Johnston D. K⁺ channel regulation of signal propagation in dendrites of hippocampal pyramidal neurons. *Nature* 1997;387:869-875.
- Hopfield JJ. 1995; Pattern recognition computation using action potential timing for stimulus representation. *Nature* 376:33-36. generation in adult rat hippocampal CA1 pyramidal cells. *J Physiol (Lond)* 1996;492:199-210.
- Jensen MS, Azouz R, Yaari Y. Spike after-depolarization and burst generation in adult rat hippocampal CA1 pyramidal cells. *J Physiol (Lond)* 1996;492:199-210.
- Kamondi A, Acsády L, Buzsáki G. Dendritic spikes are enhanced by cooperative network activity in the intact hippocampus. *J Neuroscience* 1998; in press.
- Kiss J, Buzsáki G, Morrow JS, Glantz SB, Leranth C. Entorhinal cortical innervation of parvalbumin-containing neurons (basket and chandelier cells) in the rat Ammon's horn. *Hippocampus* 1996;6:239-246.
- Konopacki J, Bland BH, Colom LV, Oddie SD. In vivo intracellular correlates of hippocampal formation theta-on and theta-off cells. *Brain Res* 1992;586:247-255.
- Laurent G. Dynamical representation of odors by oscillating and evolving neural assemblies. *Trends Neurosci* 1996;19:489-496.
- Leranth C, Frotscher M. Cholinergic innervation of hippocampal GAD⁺ and somatostatin-immunoreactive commissural neurons. *J Comp Neurol* 1987;261:33-47.
- Leung LS. Model of gradual phase shift of theta rhythm in the rat. *J Neurophysiol* 1984;52:1051-1065.
- Leung LS, Yim CY. Intracellular records of theta rhythm in hippocampal CA1 cells of the rat. *Brain Res* 1986;367:323-327.
- Leung LS, Yim CY. Intrinsic membrane potential oscillations in hippocampal neurons in vitro. *Brain Res* 1991;553:261-274.
- Leung LS, Yu H-W. Theta-frequency resonance in hippocampal CA1 neurons in vitro demonstrated by sinusoidal current injection. *J Neurophysiol* 1998, in press.
- Li X-G, Somogyi P, Tepper JM, Buzsáki G. Axonal and dendritic arborization of an intracellularly labeled chandelier cell in the CA1 region of rat hippocampus. *Exp Brain Res* 1992;90:519-525.
- Lisman JE, Idiart MAP. A mechanism for storing 7±2 short-term memories in oscillatory subcycles. *Science* 1995;267:1512-1514.
- Llinás R, Ribary U. Coherent 40-Hz oscillation characterizes dream state in humans. *Proc Natl Acad Sci USA* 1993;90:2078-2081.
- Lopes da Silva FH, Witter M, Boeijinga PH, Lohman A. Anatomic organization and physiology of the limbic cortex. *Physiol Rev* 1990;70:453-511.
- Magee JC, Johnston D. Synaptic activation of voltage-gated channels in the dendrites of hippocampal pyramidal neurons. *Science* 1995;268:301-304.
- Mitchell SJ, Ranck JB. Generation of theta rhythm in medial entorhinal cortex of freely moving rats. *Brain Res* 1980;189:49-66.
- Mitzdorf U. Current source-density method and application in cat cerebral cortex: investigation of evoked potentials and EEG phenomena. *Physiol Rev* 1985; 65:37-100.
- Nathan T, Jensen MS, Lambert JD. The slow inhibitory postsynaptic potential in rat hippocampal CA1 neurones is blocked by intracellular injection of QX 314. *Neurosci Lett* 1990;110:309-313.
- Nuñez A, Garcia-Austt E, Buno W Jr. Intracellular theta rhythm generation in identified hippocampal pyramids. *Brain Res* 1987;416:289-300.
- Nuñez A, Garcia-Austt E, Buno W. Synaptic contributions to theta rhythm genesis in rat CA1-CA3 hippocampal pyramidal neurons in vivo. *Brain Res* 1990;533:176-179.
- O'Keefe J, Nadel L. *The hippocampus as a cognitive map*. Oxford: Clarendon, 1978.
- O'Keefe J, Recce ML. Phase relationship between hippocampal place units and the EEG theta rhythm. *Hippocampus* 1993;3:317-330.
- Pedroarena C, Llinas R. Dendritic calcium conductances generate high-frequency oscillation in thalamocortical neurons. *Proc Natl Acad Sci USA* 1997;94:724-728.
- Penttonen M, Kamondi A, Sik A, Acsády L, Buzsáki G. Feed-forward and feed-back activation of the dentate gyrus in vivo: Dentate EEG spikes and sharp wave bursts. *Hippocampus* 1997;7:437-450.
- Penttonen M, Kamondi A, Acsády L, Buzsáki G. Gamma frequency oscillation in the hippocampus of the rat: Intracellular analysis in vivo. *Eur J Neurosci*, 1998;10:718-728.
- Petsche H, Stumpf C, Gogolak G. The significance of the rabbit's septum as a relay station between midbrain and the hippocampus: I. The control of hippocampus arousal activity by the septum cells. *Electroencephalogr Clin Neurophysiol* 1962;14:202-211.
- Pinsky PF, Rinzel J. Intrinsic and network rhythmogenesis in a reduced Traub model for CA3 neurons. *J Comput Neurosci* 1994;1:39-60.
- Pockberger H. Electrophysiological and morphological properties of rat motor cortex neurons in vivo. *Brain Res* 1991;539:181-190.
- Schiller J, Schiller Y, Stuart G, Sakmann. Calcium action potentials restricted to distal apical dendrites of rat neocortical neurons. *J Physiol (Lond)* 1997;503:605-616.
- Sik A, Penttonen M, Ylinen A, Buzsáki G. Hippocampal CA1 interneurons: an in vivo intracellular labeling study. *J Neurosci* 1995;15:6651-6665.

- Silva LR, Amitai Y, Connors BW. Intrinsic oscillations of neocortex generated by layer 5 pyramidal neurons. *Science* 1991;251:432-435.
- Singer W. Synchronization of cortical activity and its putative role in information processing and learning. *Ann Rev Physiol* 1993;55:349-374.
- Skaggs WE, McNaughton BL, Wilson MA, Barnes CA. Theta phase precession in hippocampal neuronal populations and the compression of temporal sequences. *Hippocampus* 1996;6:149-173.
- Soltész I, Deschênes M. Low- and high-frequency membrane potential oscillations during theta activity in CA1 and CA3 pyramidal neurons of the rat hippocampus under ketamine-xylazine anesthesia. *J Neurophysiol* 1993;70:97-116.
- Spruston N, Schiller Y, Stuart G, Sakmann B. Activity dependent action potential invasion and calcium influx into hippocampal CA1 dendrites. *Science* 1995;268:297-300.
- Steriade M, McCormick DA, Sejnowski TJ. Thalamocortical oscillations in the sleeping and aroused brain. *Science* 1993;262:679-685.
- Steriade M, Amzica F, Contreras D. Synchronization of fast (30-40 Hz) spontaneous cortical rhythms during brain activation. *J Neurosci* 1996;16:392-417.
- Stewart M, Fox SE. Do septal neurons pace the hippocampal theta rhythm? *Trends Neurosci* 1990;13:163-168.
- Thompson LT, Best PJ. Place cells and silent cells in the hippocampus of freely-behaving rats. *J Neurosci* 1989;7:2382-2390.
- Toth K, Freund TF, Miles R. Disinhibition of rat hippocampal pyramidal cells by GABAergic afferents from the septum. *J Physiol (Lond)* 1997;500:463-474.
- Traub RD, Jefferys JGR, Miles R, Whittington MA, Tóth K. A branching dendritic model of a rodent CA3 pyramidal neurone. *J Physiol* 1994;481:79-95.
- Tsodyks MV, Skaggs WE, Sejnowski TJ, McNaughton BL. Population dynamics and theta rhythm phase precession of hippocampal place cell firing: A spiking neuron model. *Hippocampus* 1996;6:271-280.
- Tsubokawa H, Ross W. IPSPs modulate spike backpropagation and associated Ca^{2+}_i changes in the dendrites of hippocampal CA1 pyramidal neurons. *J Neurophysiol* 1996;76:2896-2906.
- Vanderwolf CH. Hippocampal electrical activity and voluntary movement in the rat. *Electroencephalogr Clin Neurophysiol* 1969;26:407-418.
- Wallenstein GV, Hasselmo ME. GABAergic modulation of hippocampal population activity: Sequence learning, place field development, and the phase precession effect. *J Neurophysiol* 1997;78:393-408.
- Wang X-J. Calcium coding and adaptive temporal computation in cortical pyramidal neurons. *J Neurophysiol* 1998;79:1549-1566.
- Winson J. Patterns of hippocampal theta rhythm in freely moving rat. *Electroencephalogr Clin Neurophysiol* 1974;36:291-301.
- Wong RKS, Stewart MJ. Different firing patterns generated in dendrites and somata of CA1 pyramidal neurons in the guinea-pig hippocampus. *J Physiol (Lond)* 1992;457:675-687.
- Wong RK, Prince DA, Basbaum AI. Intradendritic recordings from hippocampal neurons. *Proc Natl Acad Sci USA* 1979;76:986-990.
- Yeckel MF, Berger TW. Feedforward excitation of the hippocampus by afferents from the entorhinal cortex: Redefinition of the role of the trisynaptic pathway. *Proc Natl Acad Sci USA* 1990;87:5832-5836.
- Ylinen A, Bragin A, Nádasdy Z, Jandó G, Szabó I, Sik A, Buzsáki G. Sharp-wave-associated high-frequency oscillation (200 Hz) in the intact hippocampus: Network and intracellular mechanisms. *J Neurosci* 1995a;14:30-46.
- Ylinen A, Soltész I, Bragin A, Penttonen M, Sik A, Buzsáki G. Intracellular correlates of hippocampal theta rhythm in identified pyramidal cells, granule cells and basket cells. *Hippocampus* 1995b;5:78-90.